Real time single and multi channel structural damage detection using recursive singular spectrum analysis

Journal Title
XX(X):2–46

DOI: 10.1177/ToBeAssigned
www.sagepub.com/
SAGE

Basuraj Bhowmik[1], Manu Krishnan[2], Budhaditya Hazra[3] and Vikram Pakrashi[4]

Abstract

A novel baseline free approach for continuous online damage detection of multi degree of freedom vibrating structures using Recursive Singular Spectral Analysis (RSSA) in conjunction with Time Varying Auto-Regressive Modeling (TVAR) is proposed in this paper. The acceleration data is used to obtain recursive proper orthogonal components online using rank-one perturbation method followed by TVAR modeling of the first transformed response, to detect the change in the dynamic behavior of the vibrating system from its original state to contiguous linear /non-linear-states indicating damage. Most work to date deal with algorithms that require windowing of the gathered data that render them ineffective for online implementation. Algorithms focussed on mathematically consistent recursive techniques in a rigorous theoretical framework of structural damage detection is missing that motivates the development of the present framework. The response from a single channel is provided as input to the algorithm in real time. The RSSA algorithm iterates the eigenvector and eigenvalue estimates for sample covariance matrices and new data point at each successive time instants. This eliminates the need for offline post processing and facilitates online damage detection especially when applied to streaming data without requiring any baseline data. Lower order TVAR models are applied on the transformed responses to improve detectability. Numerical simulations performed on a 5-dof nonlinear system and on an SDOF system modeled using a Duffing oscillator under white noise excitation data, with different levels of nonlinearity simulating the damage scenarios, demonstrate the robustness of the proposed algorithm. The method further validated on results obtained from experiments performed on a cantilever beam subjected to earthquake excitation; a toy cart experiment model with springs attached to either side demonstrate the efficacy of the proposed methodology as an appropriate candidate for real time, reference free structural health monitoring.

Keywords

Recursive Singular Spectral Analysis (RSSA), Time-Varying Autoregressive Modeling (TVAR), Damage Sensitive Features (DSFs), Structural Health Monitoring (SHM), Real time damage detection

1 Introduction

Modern society is heavily dependent on structural and mechanical systems such as aircraft, bridges, power generation systems, buildings and defence systems. A significant portion of our built infrastructure (civil and mechanical systems such as bridges, aircraft, etc.) are distressed and in need of investment, while there is inadequate and limited resources to do so (Znidaric et al. 2011). Operation, within and sometimes beyond the initially designed service life requires assessment of the ability of the system in relation to performance metrices considering ageing and degradation. This requirement leads to the need of efficient damage detection techniques in order to detect and locate the damage, estimate the severity of the damage and predict the useful remaining life of a structure. The term *structural health monitoring* (SHM) is related to the aforementioned objectives and often refers to the process of implementing damage detection strategies in structures involving the observation of a structure or mechanical system over time using periodically spaced response measurements, the extraction of damage-sensitive features from these measurements and the statistical analysis of these features to determine the current state of system health (Farrar and Worden 2007; Balageas et al. 2006; Bodeux and Golinval 2001; Worden 1997). Although damage detection strategies are well reported in literature (Balsamo and Betti 2015; Farrar and Worden 2012; Doebling et al. 1998; Nguyen et al. 2009; Yan et al. 2007; Salawu 1997), the evolution of real-time damage detection schemes capable of conducting baseline-free damage identification still remains a challenge. This is primarily due to the under-development of damage indicators capable of indicating damage instances and location of damage, simultaneously, in a single framework, and the complexities arising due to computational exhaustion that are memory and resource consuming. As the occurrence of damage can often be a real time event (Farrar and Worden 2012), changes in the damage sensitive features (DSFs) can be efficiently evaluated recursively for continuously streaming data. This paper addresses the key aspects of SHM that involves identifying the time of damage and detecting the precise location of damage in a structure in an online framework.

[1]Doctoral student, Department of Civil Engineering, Indian Institute of Technology, Guwahati, Assam, India
[2]Graduate student, Department of Civil Engineering, Indian Institute of Technology, Guwahati, Assam, India
[3]Assistant Professor, Department of Civil Engineering, Indian Institute of Technology, Guwahati, Assam, India
[4]Assistant Professor, School of Mechanical & Materials Engineering, University College Dublin, Belfield, Ireland

Corresponding author:
Budhaditya Hazra, Assistant Professor, Department of Civil Engineering, Indian Institute of Technology, Guwahati, Assam, India
Email: budhaditya.hazra@iitg.ernet.in

Prepared using sagej.cls

A majority of the damage detection schemes are offline in nature that analyze data in batches. Damage detection of structures in real time is a relatively new idea that requires significant development in the literature. Online damage detection entails identification of damage of a multi degree of freedom (MDOF) vibrating system as the recorded vibration data streams in real time. Application of system identification-based SHM strategies utilize advanced signal processing techniques (Dackermann et al. 2014) over vibration measurements gathered from a dense array of sensors (Nair et al. 2006) to monitor the condition of a structure. Numerous vibration based damage detection methods have been developed in recent years which utilize changes in modal properties such as natural frequency (Doebling et al. 1998; Salawu 1997), damping (Doebling et al. 1998; Curadelli et al. 2008) and mode shapes (Pandey et al. 1991) in order to detect damage resulting from various environmental conditions (Yan et al. 2005), human-induced excitation or natural events (Merz et al. 2004; Farrar and Worden 2012) such as earthquake (Hazra and Narasimhan 2010) and strong winds (Farrar and Worden 2012; Doebling et al. 1998). These damage detection techniques can be broadly classified as: model based methods which rely heavily on extensively calibrated finite element model (FEM) of a system (Behmanesh and Moaveni 2015; Brownjohn et al. 2001; Skolnik et al. 2006), thus rendering them computationally expensive. With increased computational cost (Behmanesh and Moaveni 2015), modeling errors (Brownjohn et al. 2001; Mottershead and Friswell 1993) and choice of model parameters (such as model order, mass, stiffness, damping parameters,etc) (Skolnik et al. 2006; Mottershead and Friswell 1993), the model-based methods are fraught with disadvantages, which limit their applications for real time damage detection. Contrary to these traditional approaches, response based methods or the non-parametric methods (Dackermann et al. 2014; Kesavan and Kiremidjian 2012; Carden and Fanning 2004; Fan and Qiao 2011; Li and Chen 2013) often overcome the aforementioned limitations by utilizing advanced signal processing techniques in conjunction with vibration measurements to monitor the condition of a structure. This category of methods rely on vibration data to extract features related to a change at the onset of damage, thereby implementing a real time damage detection strategy tailored towards an online framework.

The use of data driven techniques developed in the field of classical time series analysis (Sadhu and Hazra 2013; Mirmomeni et al. 2013), multi-variate statistics (Misra et al. 2002) and signal processing (Fan and Qiao 2011; Hazra and Narasimhan 2010) ranging to diverse applicabilities like system identification, tool wear detection and missing data recovery, show great potential in finding key patterns for appropriate prediction of such series (Hassani 2010; Golyandina and Zhigljavsky 2013). Singular spectrum analysis (SSA) (Hassani 2010), a powerful technique developed in recent years, utilizes the key concept of separability for decomposition (Hassani 2010) and reconstruction of the time

series (Hassani 2010; Golyandina and Zhigljavsky 2013) in two separate steps, without any statistical assumptions such as stationarity of the series or normality of the residuals. Due to the methodological stress on separability of one component of the series from another one, the assumption of stationarity is not required, making the algorithm amenable towards applicability for non-stationary time series as well. A useful tool in the predicting trends in time series, SSA can be used to address problems related to smoothing, extraction of seasonality components, optimal filtering and analysis of seismic signals, by using basis functions characterized by its data-adaptive nature. This makes the approach extended to the analysis of nonlinear aspects (Elsner and Tsonis 2013). SSA decomposes a given time series into a set of additive time series and separates a multi-frequency signal into its mono-components. Using of principal component analysis (PCA), the method projects an original time series onto a vector basis obtained from the series itself. In this process, the set of these series can be seen as a slowly varying trend representing the signal mean at each instant. As a result, noise which can be filtered from the original data set together with the special features of the structure expressed by vibration signals can be extracted (Golyandina and Zhigljavsky 2013).

The development of online damage detection techniques based on processing of response streaming in real time, still remains a challenge. The main motivation behind the present work is to develop a damage detection framework which can process data online and detect damage in a structure in real time. Applications involving aging and wearing out of components, processes dealing with seismic signals, are generally time-varying where the signals evolve in real time and the process becomes too complex to be analyzed via a simple offline method (Misra et al. 2002; Yu et al. 2013; Gharibnezhad et al. 2015). In practical SHM scenarios, data streams continuously in real time, which further necessitates that the algorithm should be amenable towards online implementation, independent of any baseline ~~(reference)~~ data. Traditional SSA requires a batch of data to elicit principal components (PCs) of the original time series, via eigen-decomposition of the covariance matrix, that solely works offline. This hinders its performance when applied to time-varying and non-stationary processes (Hassani 2010; Golyandina and Zhigljavsky 2013). In this paper, a baseline free approach has been proposed which facilitates the monitoring of structural systems directly using acceleration data, utilizing the concepts of recursive singular spectrum analysis (RSSA) (Mirmomeni et al. 2013), as a tool for real time processing of data. The proposed method uses first-order perturbation (FOP) approach for the sample covariance matrix estimate with every new sample obtained in real time. Whereas the traditional SSA approach processes chunks of data acquired in batch mode, RSSA provides online processing of data based on rank one eigenvector updates in a recursive framework, as and when the data streams in real time (Mirmomeni et al. 2013; Hassani et al. 2013). It should be noted that the data covariance matrix should

be strictly diagonally dominant at any instant of time, for the algorithm to work online, which is automatically satisfied by structural dynamical systems with low to moderate damping. Once the eigenspace updates are obtained, an approximation of the original time series is carried out by reconstruction, leaving the random (noise) components behind, where the framework then utilizes time-varying autoregressive (TVAR) modeling in conjunction with DSFs for identifying the instant of damage (Hassani 2010; Mirmomeni et al. 2013).

Time series models work extremely well in capturing the key features of any data series, thus finding application in monitoring structural condition and detection of damage using time varying coefficients, without resorting to spectral representation. Analysis of coefficients of autoregressive (AR) model (Farrar and Worden 2007; Sadhu and Hazra 2013), autoregressive with exogenous input (ARX) model, autoregressive moving average model (ARMA), autoregressive moving average with exogenous input (ARMAX) model, are some of the noteworthy aspects of traditional damage detection schemes extensively developed in literature (Sadhu and Hazra 2013; Nair et al. 2006). An inherent drawback of these methods is the fact that the methods are not receptive towards online implementation for a continuous real time streaming of data. To tailor the basic AR modeling used in this paper towards recursive implementation and to better capture the non-stationarity involved with the data due to the damage induced in the structure, the authors have resorted to TVAR modeling, which is utilized to obtain the coefficients in real time to track the changes, indicative of an onset of damage (Musafere et al. 2015). A shortcoming in the implementation in the proposed method is to pre-select the model order required to implement the current framework. In the proposed method, TVAR modeling is applied on the reduced responses obtained from the RSSA algorithm, rather than the raw vibration responses, which allows a relatively low order time-series model capture the dynamics of the structure in a recursive framework. The proposed framework, essentially exclusive of baseline data, facilitates simultaneous spatio-temporal damage detection of a structure in real time, through the monitoring of the time varying coefficients of the TVAR models.

The main contributions of this work are as follows: **First,** a novel framework has been provided using RSSA as a structural damage detection tool that works in real time as the data streams in. To the best knowledge of the authors, concepts utilizing RSSA in the purview of structural damage detection has so far not been explored. **Secondly,** damage can be inferred using TVAR model on the reduced order response obtained from RSSA algorithm in the order of about 15% for both global damage and for local damage cases. This level of damage has not been reported in literature so far. **Thirdly,** simultaneous spatial and temporal damage detection using a single framework is difficult. The key idea of this work is to detect spatio-temporal damage in real time, which is accomplished by using iterative DSFs on the

TVAR modeling, shown in the subsequent sections. **Finally**, the authors have extended the utility of the proposed algorithm to asses damage detection using multi channel singular spectrum analysis (MSSA) which is capable of identifying the dominant patterns in time as well as space. The proposed method is applied for damage detection in a 5 dof system that is modeled as a 4 storied linear stiffness structure with a Bouc-Wen (B-W) base at the model and a single storey modeled with a Duffing oscillator at its base. These numerical results were complemented with experimental tests involving a toy-cart setup modeled as a single degree of freedom system (SDOF) attached to six springs, three on either side of the mass, excited using ground motion on an actuator table. Additionally, the authors have provided a separate experimental verification involving a cantilever beam model fixed to a base plate on a shake table and excited using ground motions of varying intensities to detect damage based on the nonlinearity provided by a rubber strip attached to the free end of the beam.

The paper is organized as follows. First, a brief description of RSSA is presented in the framework of structural dynamics. Then, damage detection using DSFs is provided, with a background of the time series concepts used herein. The proposed algorithm is demonstrated with the aid of numerical examples and the corresponding results are provided. Finally, the proposed method is complemented using data obtained from experimental setups carried out in laboratory environment which demonstrate the efficiency and the robustness of the algorithm in practical situations.

2 Background

SSA is a non-parametric method that works well with arbitrary statistical processes and requires no prior assumptions about the stationarity, linearity or normality of the data set. Somewhat similar to PCA based methods (Kesavan and Kiremidjian 2012), SSA projects the original time series into a smaller dimensional space which is composed of lagged signal components, while retaining most of the variance and the information associated with the particular data set (Hassani 2010; Liu et al. 2014). The most prominent difference between the methods is that while in PCA, the singular value decomposition (SVD) is carried out predominantly on data sets obtained from sensors spatially located on the system, SSA extracts the time history data obtained from each sensor and utilizes SVD on the Hankel matrix formed by the streaming data (Hassani 2010). PCA re-expresses the original data into a transformed state of uncorrelated variables and estimates the covariance updates of the dataset in growing windows or in batches. The superiority of SSA over the basic classical approaches is that the method decomposes a series into its component parts and reconstructs the series by leaving out the random (or noise) component behind. To tailor the traditional SSA method towards online implementation, an extension premised mainly on first order perturbation techniques, known as RSSA, is proposed in this paper, that enables

online spatio-temporal damage detection in a single framework (Mirmomeni et al. 2013; Hassani et al. 2013).

2.1 Basic SSA

The main objective of SSA is to decompose the original time series into a set of mono-component signals from which three different characteristics can be extracted, namely- *slowly varying trend*, *harmonic* (or *oscillatory*) component and *noise*. According to Golyandina (Golyandina and Zhigljavsky 2013), trend components correspond to slow varying additive component of the series in which the oscillations are removed or smoothed. The harmonic series are periodic in nature which are either pure or amplitude modulated, while the noise component is any aperiodic series that does not affect the performance and/or functioning of the algorithm since it is removed during the reconstruction of the time series. The algorithm creates a Hankel matrix out of the time series itself by sliding a window that is shorter than the length of the time series. This process is known as *embedding*. The matrix is then decomposed into a number of elementary matrices of decreasing norm, through the process of *singular value decomposition* (SVD). *Grouping* is done by truncating the summation of the elementary matrices to yield an approximation of the original matrix, neglecting the irrelevant matrices which hardly contribute to the norm of the original matrix. This results in an approximated time series which is computed by taking the average of the diagonals, known as *reconstruction* or *diagonal averaging*. The above description is further explained through the following steps (Hassani 2010; Golyandina and Zhigljavsky 2013):

Step 1: *Embedding*

Consider a multi-dimensional sequence $X(t)$ composed of vectors that indicate measurements from each sensor. The number of rows of the matrix indicate the number of sensors corresponding to each dof used for measuring the output vibration data, while the number of columns denote the recorded data at each discretized sample point. A multi dimensional sequence $\{X(t)\}$ is extracted from the original time series into a multi dimensional series of L-lagged vectors $(X_1, X_2, ..., X_k)$, where L represents the window length and $K = T - L + 1$, where T corresponds to the number of sample points. The result of this step is the trajectory matrix $\mathbf{X} = [\mathbf{X}_1, ..., \mathbf{X}_K]$, the elements of which are given as :

$$\mathbf{X} = \begin{pmatrix} X_1 & X_2 & X_3 & \dots & X_K \\ X_2 & X_3 & X_4 & \dots & X_{K+1} \\ X_3 & X_4 & X_5 & \dots & X_{K+2} \\ \vdots & \vdots & \vdots & \ddots & \vdots \\ X_L & X_{L+1} & X_{L+2} & \dots & X_T \end{pmatrix} \tag{1}$$

The result of this step is a Hankel matrix. The one time-dimensional time series is converted to a multi dimensional series using a moving window of constant length. The choice of window parameters depends on the characteristics of data-set.

Step 2: *SVD on the Hankel matrix*

The application of SVD on the Hankel matrix formed from the previous step has its roots in basic PCA. PCA is a linear orthogonal transformation that maps a set of physical variables to a new set of uncorrelated transformed variables, thereby resulting in reducing a complex data set to a lower dimension to reveal some hidden and simplified structures associated with the data set. PCA, in the present context is carried out by performing an eigen value decomposition (EVD) on the Hankel covariance matrix, $\mathbf{C}_X = \frac{1}{N}\mathbf{X}\mathbf{X}^T$, where the superscript "T" indicates the transpose of the matrix. Let the EVD of the Hankel covariance matrix be written as $\mathbf{C}_X = \mathbf{U}\Upsilon\mathbf{U}^T$, where U represents the eigen vectors arranged row-wise and Υ represents the diagonal matrix of eigen values in their descending order of significance.

Step 3: *Eliciting principal components of the Hankel matrix*

Principal components are obtained by projecting the Hankel matrix onto the eigenvectors, thereby transforming the data set onto a new subspace. Let U_i represent the eigenvector corresponding to Υ_i eigen value. Selection of PCs is based on the relative order of significance of eigen values. Principal component corresponding to a particular eigen vector is obtained as

$$\psi_i = (U_i^T)_{1\times L}(\mathbf{X})_{L\times K} \tag{2}$$

Once all the PCs are obtained, they can be arranged in a matrix of principal orthogonal components (POCs) as below

$$\mathbf{\Psi} = [\psi_1, \psi_2, \ldots\ldots\ldots \psi_L]^T \tag{3}$$

Step 4: *Reconstruction of the Hankel matrix and the time series*

The Hankel matrix may be expressed as the summation of d rank one elementary matrices as $\mathbf{X} = \mathbf{R_1} + \mathbf{R_2} + \ldots\ldots\mathbf{R_n}$, where n represents the number of non-zero eigen values in the Υ_i matrix. It should also be noted that the n elementary matrices are selected according to their relative order of significance as given by the decreasing order of their corresponding eigen values. The basic aim of this step is to reconstruct the Hankel matrix and thereby the original time series only using the PCs that explain maximum variance. This ensures elimination of noise and unwanted components from the time series, which further warrants the usage of a low model order in the succeeding steps. The elementary

matrices are obtained by projecting the PCs back into the original eigen space as shown below:

$$\begin{aligned} \mathbf{R}_i &= U_i \times \psi_i \\ \mathbf{X} &= \sum_{i=1}^{n} \mathbf{R}_i \end{aligned} \tag{4}$$

The Hankel matrix can now be reconstituted as per the equation (4). The reconstituted trajectory matrix is an approximated version of the original matrix and the approximated time series is recovered by taking the average of the diagonals. Let x_{ij} be the elements of the Hankel matrix , where i denotes the row number and j the column number. Considering $L^* = min(L, K)$, $K^* = max(L, K)$ and $N = L + K - 1$, it could be assumed that, x^*_{ij}=x_{ij} if $L < K$ and x^*_{ij}=x_{ji}, otherwise. The individual elements of the time series X_k is obtained using the following equations (Hassani 2010; Golyandina and Zhigljavsky 2013):

$$x_k = \begin{cases} \frac{1}{k+1} \sum_{m=1}^{k+1} {x^*}_{m,k-m+2} & for \quad 0 \leq k < L^* - 1 \\ \frac{1}{L^*} \sum_{m=1}^{L^*} x^*_{m,k-m+2} & for \quad L^* - 1 \leq k < K^* \\ \frac{1}{T-k} \sum_{m=k-K^*+2}^{T-K^*+1} x^*_{m,k-m+2} & for \quad K^* \leq k \leq T \end{cases} \tag{5}$$

From the formulations involved, it is clear that the regular SSA requires a batch of data. These data provide a covariance matrix via the trajectory matrix of the signal in an offline framework. By the subsequent application of SVD on the covariance matrix the PCs of the time series are elicited. This part requires exhaustive matrix operations and makes the SSA unsuitable for online applications.

2.2 Recursive singular spectrum analysis (RSSA)

The main disadvantage of traditional SSA is that it analyzes data in batches, offline. Recent research in signal processing and information technology has identified SSA as an efficient damage detection tool (Mirmomeni et al. 2013; Hassani et al. 2013), leading to the development of SSA based structural damage detection algorithms (Chao and Loh 2014; Lakshmi et al. 2016). The major challenge towards tailoring SSA towards an online implementation is to perform the EVD of the Hankel covariance matrix at each time instant, which can be time consuming, thereby impeding its practical applicability towards real time damage detection. This can be alleviated through the use of first order perturbation approach (FOP) (Krishnan et al. 2017a; Li et al. 2000) which provides recursive updates of eigen subspace from

the previous eigen-space of the data at a particular time instant.
The recursive estimation of the Hankel covariance matrix ($\mathbf{C}_k$) at any instant k can be structured in terms of the current sample vector (X_k) and the previous covariance estimates ($\mathbf{C}_{k-1}$) as follows :

$$\mathbf{C}_k = \frac{k-1}{k}\mathbf{C}_{k-1} + \frac{1}{k}X_k X_k^T \tag{6}$$

The current L dimensional sample vector ($X_k = [x_{k-L+1}, x_{k-L+2}, x_{k-L+3}, ...x_k]^T$) comprises of L lagged elements of the one dimensional time series, L being the initial signal length. The objective of pre-selecting a desired initial signal length is to preserve the components with most of the damage information (by selecting components with higher singular values to retain the trend and oscillatory parts) and to eliminate the components of less significance such as noise (Mirmomeni et al. 2013). The covariance estimate at k^{th} instant can be written in terms of eigen value and eigen vector matrix at a particular time instant as $\mathbf{C}_k = \mathbf{U}_k \Upsilon_k {\mathbf{U}_k}^T$ with $\varpi_k = \mathbf{U}_{k-1}^T \mathbf{X}_k$, as the projection of the sample vector into the previous eigen subspace. Substituting these expressions in equation (6), the following equation is obtained:

$$\begin{aligned}\mathbf{U}_k(k\Upsilon_k)\mathbf{U}_k^T &= (k-1)\mathbf{U}_{k-1}\Upsilon_{k-1}\mathbf{U}_{k-1}^T + \varpi_k\varpi_k^T\mathbf{U}_{k-1}\mathbf{U}_{k-1}^T \\ &= \mathbf{U}_{k-1}\{(k-1)\Upsilon_{k-1} + \varpi_k\varpi_k^T\}\mathbf{U}_{k-1}^T\end{aligned} \tag{7}$$

In the above expression, with ~~a~~ finitely large sample size (k) and low damping estimates (Krishnan et al. 2017a), the term $((k-1)\Upsilon_{k-1} + \varpi_k\varpi_k^T)$ generally shows a diagonally dominant behavior. The diagonal dominant structure of this term ensures the application of Gershgorin's theorem (Golub and Van Loan 2012), rendering in the application of FOP approach admissible to obtain the eigen values and eigen vectors. Interested readers could refer (Krishnan et al. 2017a; Li et al. 2000) for details. The application of Gershgorin's theorem ensures the EVD of the term to be of the form $\mathrm{P}_k\mathbf{\Gamma}_k\mathrm{P}_k^T$, where $\mathbf{P}$ is orthonormal and $\mathbf{\Gamma}$ is diagonal. Substituting the EVD in place of $((k-1)\Upsilon_{k-1} + \varpi_k\varpi_k^T)$ in equation (7), a new formulation is obtained as shown below:

$$\mathbf{U}_k(k\Upsilon_k)\mathbf{U}_k^T = (\mathbf{U}_{k-1}\mathrm{P}_\mathbf{k})\mathbf{\Gamma_k}(\mathrm{P}_\mathbf{k}^\mathbf{T}\mathbf{U}_{\mathbf{k-1}}^\mathbf{T}) \tag{8}$$

From equation (8), recursive updates of the eigen subspace are obtained as a function of the previous eigen space as:

$$\begin{aligned}\mathbf{U_k} &= \mathbf{U}_{k-1}\mathrm{P}_\mathbf{k} \\ \Upsilon_k &= \mathbf{\Gamma}_k/k\end{aligned} \tag{9}$$

Equation (9) provides an iterative relation between eigen spaces at consecutive time instants. On using FOP approach, the recursive eigen vectors obtained at each time instants are not ordered in the same sequence as the previous time instant, thus presenting the problem of permutation ambiguity. This can be resolved by arranging the obtained eigen vectors according to the decreasing order of the corresponding eigen values in $\mathbf{\Gamma}_k$. For the working of RSSA algorithm, this is one of the key steps as eigen values of the covariance Hankel matrix need to be ordered before proceeding with the evaluation of PCs and reconstruction of Hankel matrix using them. The contribution factor for a particular i^{th} eigen vector U_i is given by $\frac{\beta_i^2}{\sum_{i=1}^{n} \beta_i^2}$, where β_i^2 is the eigen value corresponding to U_i. After obtaining the eigen space updates at a particular time instant from the previous eigen space and current sample vector, principal component values of the time series at a particular time series can be extracted as below:

$$\psi_i(k) = (U_i^T(k))_{1\times L}(\mathbf{X}_k)_{L\times 1} \tag{10}$$

Using the above equation, the i^{th} principal component value at particular time instant is obtained. Depending upon the relative contribution of the eigen vectors, the number of PCs required for reconstruction can be automated. For the present work, at any instant k, the PCs of eigenvectors that explain more than 90% of the system's variance is used for reconstruction. In the reconstruction step, the i^{th} PCs are projected back into its original subspace to obtain last column of the corresponding elementary matrix.

$$\mathbf{R}_i(k) = (U_i(k))_{L\times 1} \times (\psi_i(k))_{1\times 1} \tag{11}$$

It is to be noted here that the last entry of the $\mathbf{R}_i(k)$ vector, denoted here as $r_i(k)$ is used to obtain the value of the reconstructed time series entry at the k^{th} instant of time as shown below:

$$x(k) = \frac{1}{n}\sum_{i=1}^{n} r_i(k) \tag{12}$$

where n denotes the number of eigen values explaining more than 90% of the variance. The reconstructed signal values as per equation (12) is recursively obtained at each instant of time as and when the vibration data streams in. The importance of this reconstructed signal is that it has a near mono component nature making it amenable towards a lower AR order model, deemed sufficient (Sadhu and Hazra 2013; Krishnan et al. 2017b) to capture the dynamics of the structure and more sensitive towards singular events like damage. TVAR modeling is subsequently performed on this reconstituted signal.

3 Recursive Damage Indices

In the present framework, RSSA facilitates online processing of data producing recursive updates of eigen vectors and eigen values, referred to as eigen subspace. The eigen subspace by themselves cannot detect the change in system properties inflicted due to damage, if not processed by a set of damage markers commonly referred to as damage sensitive features (DSFs) (Hazra and Narasimhan 2010). The primary requirements of good DSFs are their ability to detect the presence of damage, effectively distinguish between the damaged and undamaged states of the structure, followed by their capacity to possibly locate and quantify the extent of damage. Additionally, to detect damages in real time, the proposed DSFs should be amenable towards online implementation and should accurately identify the presence of damage as and when the response data streams in continuously. Several damage detection and SHM techniques have been proposed in the literature (Farrar and Worden 2007) that involve use of specific DSFs whose changes signify damage to the system. The disadvantages associated with traditional DSFs includes requirement of (**i**) baseline or reference data from a healthy structure; (**ii**) windowing of response data, etc., which impedes their application in an online framework. In this section, a brief background on the formulation of *online DSFs* is proposed utilizing the concepts of TVAR coefficients and recursive signal statistics. These features are based on the reorientation of eigen-space due to damage manifested in the form of change in the pattern of TVAR modeling before and after damage. In the following sections, TVAR coefficients (a_i), and eigen ratio difference (ERD) for damage detection, are presented.

3.1 Time varying auto-regressive coefficients

The key DSF utilized in the paper are the TVAR coefficients. The motivation for this DSF is derived from the use of AR coefficients as a criterion for novelty evaluation (Gul and Catbas 2009), which presents the use of a statistical parameter known as Mahalanobis distance applied on AR coefficients to distinguish between a damaged state and an undamaged state. In order to characterize the behavior of the POC updates (which can be approximated to normal coordinates), TVAR modeling is adopted here (Musafere et al. 2015). The use of TVAR modeling for detecting structural damages has been attempted in the recent times with a fair amount of success (Hazra et al. 2016). TVAR coefficients of the modeled transformed response are tracked in real time in order to identify the damage instant. However, estimation of these coefficients frequently requires the use of windowing and baseline data to detect damage, making online implementation difficult. These drawbacks motivate the need of using a TVAR modeling based framework (Hazra et al. 2016) which does not involve any baseline to detect damage in real time, enabling it to capture the non stationary nature associated the data due to damage. The

proposed method tracks the TVAR coefficients in real time, which are used to ascertain damage induced in the structure by a change in the mean level of the plot, at the exact instant of damage. The sudden changes in TVAR coefficients indicate the alterations in the dynamical properties of the system, such as shifts in natural frequencies, changes in the mode shapes of the system, etc., induced due to damage in the system. In the proposed work, the transformed response (i.e.,the first POC) extracted from the RSSA algorithm is modeled using a TVAR model. However, the main drawback associated with using TVAR models is the selection of model order apriori such that the resulting TVAR model correctly characterizes the data during the times of interest. The use of POCs instead of the raw vibration data, whose near resemblance to normal coordinates enables the use of a low model order, resolves the issue of model order selection. The near mono-component nature of the transformed response ensures that low model order is sufficient to capture its dynamics; therefore, in the proposed framework, a model order of 2 (two) is pre-selected for all cases.

Let $X(k)$ represent the reconstructed signal at any instant which captures the maximum kinetic energy of the system and let $V(k)$ denote a zero mean Gaussian white noise with variance σ_v^2. Then the AR model of order p can be represented as:

$$X\left(k\right)=\sum_{i=1}^{p}a_{i}X\left(k-i\right)+V\left(k\right) \tag{13}$$

For real time implementation of AR model and also to make it robust against nonstationarities that might be encountered in real life data (e.g. earthquake excitation, real time occurrence of damage, etc.), the POCs are modeled using TVAR modeling in which $a_i's$ are a function of time. For this purpose, the Kalman filter is utilized to estimate these time-varying coefficients (Hazra et al. 2016). The following equation is the discrete representation of the $a_i(t)$ coefficients and $W(k)$ is the process noise with variance σ_w^2 and covariance, $\mathbf{P_w}=\mathbf{I_{p\times p}}\boldsymbol{\sigma}_{\mathbf{w}}^{\mathbf{2}}$. Both noise measurements $V(k)$ and $W(k)$ are mutually independent and uncorrelated. Consider the following set of equations, where the unknown state vector $B(k)$ is expressed as shown:

$$\begin{aligned}B(k)&=\Gamma(k-1)B(k-1)+W(k)\\X(k)&=\mathbf{C(k)}B(k)+V(k)\end{aligned} \tag{14}$$

The state vector $B(k)$ is given by: $B\left(k\right)=\left[a_1\left(k\right),a_2\left(k\right),\ldots\ldots a_p\left(k\right)\right]^T$. The matrix $\mathbf{\Gamma}(k-1)$ is an identity matrix ($\mathbf{I}_{p\times p}$). The matrix C_k is the observation data with discrete k steps given as: $\mathbf{C}\left(k\right)=\left[X\left(k-1\right),X\left(k-2\right)\ldots\ldots X\left(k-p\right)\right]$. The Kalman filter has mainly two processes: one is the

stepwise time update (prediction) and the other one is measurement update (correction) of the predicted data. At each step, the set of the Kalman filter equations can be written as (Bodeux and Golinval 2001; Hazra et al. 2016)

$$\begin{aligned} B\left(k|k-1\right) &= B\left(k-1|k-1\right) \\ \mathbf{P}_b\left(k|k-1\right) &= \mathbf{P}_b\left(k-1|k-1\right) + \mathbf{I}\sigma_w^2 \\ \psi^1\left(k|k-1\right) &= \mathbf{C}\left(k\right) B\left(k|k-1\right) \\ \sigma_x^2\left(k|k-1\right) &= \mathbf{C}\left(k\right) \mathbf{P}_b\left(k|k-1\right) \mathbf{C}(k)^T + \sigma_v^2 \end{aligned} \tag{15}$$

And,

$$\begin{aligned} \mathbf{KG}\left(k\right) &= \mathbf{P}_b\left(k|k-1\right) \mathbf{C}(k)^T \sigma_x^2(k|k-1)^{-1} \\ B\left(k|k\right) &= B\left(k|k-1\right) - \mathbf{KG}\left(k\right)\left[X\left(k\right) - X\left(k|k-1\right)\right] \\ \mathbf{P}_b(k|k) &= \left[\mathbf{I} - \mathbf{KG}(k)\mathbf{C}(k)\right]\mathbf{P}_b(k|k-1)\right] \end{aligned} \tag{16}$$

where $B\left(k|k-1\right)$ represents apriori estimate and its linear combination would result in $B\left(k|k\right)$, which is aposteriori. The Kalman Gain $\mathbf{KG}(k)$ gives a weightage to the prediction error $X\left(k\right) - X\left(k|k-1\right)$, to minimize the state estimation error $B\left(k|k\right)$. The apriori and the posteriori covariance estimates are given by $\mathbf{P}_b\left(k|k-1\right)$ and $\mathbf{P}_b\left(k|k-1\right)$, respectively. Although the TVAR model facilitates adequate representation of the non stationary transformed response, however, in order to use it for damage detection, the TVAR model alone is not enough. Consequently, DSFs are applied on the TVAR coefficients to detect damage to detect damage which run in real time. The basic equation 13 therefore, becomes:

$$X\left(k\right) = a_1(k)X\left(k-1\right) + a_2(k)X\left(k-2\right) + V\left(k\right) \tag{17}$$

where, $X(k)$ represents the POC at any instant that captures the maximum variance of the system. Although a_1 and a_2 are expected to alter mildly at each time instants due to a drift in the post damage values from the pre-damage values, the damage instant is characterized by sudden changes in the overall behavior of TVAR coefficients. The change in a_1 and a_2, tracked recursively, serves as an indicator of damage.

3.2 Damage detection using recursive eigen ratio difference

In the present work, the ratio of two singular values, quantifying the coupling level between two singular values in RSSA, is utilized as a secondary DSF. The use of this quantity as a possible indicator of instability was first adopted for monitoring volcanic activity (Carniel et al. 2006). The principle behind the use of this marker is that structural damage or instability induces a low frequency component in the signal, creating a de-coupling between the two most significant PCs. This decoupling, can intuitively be represented in the form of ratio between their corresponding singular values or eigen values. This

concept of decoupling has been utilized in the present work to formulate an online damage index known as recursive eigen ratio difference to accurately identify the instant of damage, which is given as below:

$$\delta(k) = \left[\frac{(\lambda_1(k) - \lambda_2(k))}{\sum_{i=1}^{L} \lambda_i} \right] \tag{18}$$

At the instant of damage, recursive ERD shows an alteration in its mean level to indicate the decoupling between the two most significant singular values. The potential of ERD to be implemented online towards damage detection demonstrates its capability to detect damage even for cases of a non-stationary nature of input data. ERD when examined in a recursive framework supplements the use of AR coefficients as an effective damage detection tool for the proposed framework. This is shown at a later stage of the manuscript.

4 Multichannel singular spectrum analysis (MSSA)

This section describes the basic multichannel singular spectrum analysis (MSSA) and its recursive implementation, suitable for online implementation. MSSA is a data-driven technique arising from research on alternative tools for the analysis of multichannel time series and can be considered as a natural extension of the basic SSA algorithm (Rangelova et al. 2012). SSA, albeit being an efficient algorithm for extracting the principal patterns in time, becomes computationally demanding for structures with significantly large number of DOF (e.g. UCLA Factor Building (UCLAFAC), (Krishnan et al. 2017a)). MSSA uses a multivariate time series with all state variables of the coupled systems in the construction of the augmented trajectory matrix. Literature in MSSA (Rangelova et al. 2012; Hsieh and Wu 2012) shows that the variable chosen to analyze the system will have significant impact on the robustness of the algorithm to capture the dynamics of the system under study. The conventional eigen vector or PCA is a special case of the MSSA when no time lags are introduced. According to Richman (Richman 1986), the eigen vectors show distortions that contribute to inaccurate representation of the physical relationships in the data. In the presence of data gaps in the data series, the resulting modes of the decomposition of the data are not strictly orthogonal (Venegas et al. 1997).

Consider the multivariate time series of length N and D channels, $\mathbf{x} = \{\mathbf{x}_n^d : d = 1, ...D; n = 1, ...N\}$. Similar to SSA, the first step of MSSA algorithm is to create an augmented trajectory matrix with data from the concerned channels. Each channel d is embedded into an L dimensional phase space by using lagged replicates $X_1^i, X_2^i, ..., X_k^i$, where i ranges from 1 to D, D being the number of channels considered for MSSA. Hence if there are D channels, each embedded into an L dimensional phase space

system, the number of rows of the augmented matrix will be $L \times D$ and number of columns will be $K = N - L + 1$. The structure of the trajectory matrix is as shown below:

$$\mathbf{X}_D = \begin{bmatrix} \underbrace{\begin{matrix} x_1^1 & x_2^1 & x_3^1 & . & x_L^1 \\ x_2^1 & x_3^1 & x_4^1 & . & x_{L+1}^1 \\ . & . & . & . & . \\ . & . & . & . & . \\ x_K^1 & x_{K+1}^1 & x_{K+2}^1 & . & x_N^1 \end{matrix}}_{Channel-1} & \underbrace{\begin{matrix} x_1^2 & x_2^2 & x_3^2 & . & x_L^2 \\ x_2^2 & x_3^2 & x_4^2 & . & x_{L+1}^2 \\ . & . & . & . & . \\ . & . & . & . & . \\ x_K^2 & x_{K+1}^2 & x_{K+2}^2 & . & x_N^2 \end{matrix}}_{Channel-2} & . . . & \underbrace{\begin{matrix} x_1^D & x_2^D & x_3^D & . & x_L^D \\ x_2^D & x_3^D & x_4^D & . & x_{L+1}^D \\ . & . & . & . & . \\ . & . & . & . & . \\ x_K^D & x_{K+1}^D & x_{K+2}^D & . & x_N^D \end{matrix}}_{Channel-D} \end{bmatrix}^{\mathbf{T}} \tag{19}$$

The formulation for MSSA are similar to the steps provided in Section 2.1, for a basic SSA algorithm. Applying SVD on the augmented trajectory covariance matrix yields $L \times D$ eigen values and eigen vectors. As the number of channels increases, MSSA becomes computationally expensive. However, MSSA shows good results in interpreting damage events, which is illustrated in the later parts of the study. Hence, projecting the dataset onto the eigenvectors simplifies the picture of a possibly high-dimensional complex system by viewing it in an optimal subspace (Groth and Ghil. 2015). It is well understood that there will be D sets of $L \times L$ eigen value matrix and eigen vector matrix. Consequently, there will be D sets of L PCs, each accounting for correlation between different data sets taken as input to the algorithm. For TVAR modeling, only one signal is required, but MSSA algorithm gives D reconstructed signals as output. Hence, to tailor the basic MSSA algorithm towards damage detection using TVAR modeling, the authors suggest utilizing the first two PCs of every D channels, towards building a composite signal that accounts for all the D input channels. The composite signal contains the maximum information to aid towards the detection problems, obtained using the most significant PCs. Let $\mathbf{\Psi}_D = \left[\psi_1^1, \psi_2^1, ...\psi_L^1, ..., \psi_1^D, \psi_2^D, ...\psi_L^D\right]^{\mathbf{T}}$ represent the PCs obtained from Step 3 as mentioned in Section 2.1. Using only the first two PCs of each channel, the trajectory matrix is reconstructed as below:

$$\mathbf{R}_i = \frac{\left\{ \sum_{j=1}^{D} \sum_{i=1}^{2} U_i^j \times \psi_i^j \right\}}{D} \tag{20}$$

The composite signal from the trajectory matrix is obtained using the same diagonal averaging as explained in equation (5). The reconstructed composite signal has the maximum information contained towards TVAR modeling and subsequent damage detection. The signal is generated based on the principal components containing the maximum variance, in each channel.

4.1 Recursive multichannel singular spectrum analysis (RMSSA)

The main disadvantage of MSSA algorithm is that when the number of channels increases, it becomes computationally more involved. This becomes an impeding factor even for developing a recursive version of basic MSSA algorithm towards processing real time multi degree of freedom data. The authors have made an attempt to develop a recursive version of MSSA algorithm in this paper by modifying the basic RSSA algorithm to account for multiple input channels, which is a key entitlement of the paper. Following the similar lines of development, as in equation (6), the RMSSA algorithm can be proposed as follows:

$$C_k = \frac{k-1}{k} C_{k-1} + \frac{1}{k} \widetilde{X}_{k_D} \widetilde{X}_{k_D} \tag{21}$$

where $\widetilde{X}_{k_D} = \left[x^1_{k-L+1}, x^1_{x-L+2}, x^1_{x-L+3} \ldots\ldots\ldots x^1_k, \quad x^2_{k-L+1}, x^2_{x-L+2}, x^2_{x-L+3} \ldots\ldots\ldots x^2_k, \ldots\ldots, x^D_{k-L+1}, x^D_{x-L+2}, x^D_{x-L+3} \ldots\ldots\ldots x^D_k\right]^T$

Once the recursive equation is ready, all the other steps from equation (7) to equation (12) follows. The key steps of the formulation include the updating of the covariance matrix formed at each time stamp and providing eigen decomposition so as to tailor the basic MSSA algorithm towards its recursive version. Similar to the previous approach of deriving the RSSA equations, the eigen decomposition of the covariance matrix at the k^{th} time instant could be written as $\mathbf{C}_k = \mathbf{W}_k \Omega_k \mathbf{W}_k^T$. On substituting to the covariance update equation 21, with $\beta_k = \mathbf{W}_{k-1} \tilde{X}_{k_D}$, and performing simple algebraic calculations, the following equation is obtained:

$$\mathbf{W}_k \Omega_k \mathbf{W}_k^T = \mathbf{W}_{k-1} \left[(k-1)\, \mathbf{\Omega}_{k-1} + \beta_k \beta_k^T \right] \mathbf{W}_{k-1}^T \tag{22}$$

For finitely large samplesize k and low damping estimates (Krishnan et al. 2017a), the term $((k-1)\Omega_{k-1} + \beta_k \beta_k^T)$ generally shows a diagonally dominant behavior. The diagonal dominant structure of this term ensures the application of Gershgorin's theorem, rendering in the application of FOP approach admissible to obtain the eigen values and eigen vectors (Krishnan et al. 2017a; Li et al. 2000). The application of Gershgorin's theorem ensures the EVD of the term to be of the form $\mathrm{T}_k \mathbf{\Lambda}_k \mathrm{T}_k^T$, where $\mathbf{T}$ is orthonormal and $\mathbf{\Lambda}$ is diagonal, similar to the previous approach. Substituting the EVD in equation (22), the covariance matrix update could be simplified as follows:

$$\mathbf{W}_k k \Omega_k \mathbf{W}_k^T = (\mathbf{W}_{k-1} \mathbf{T}_k)(\mathbf{\Lambda}_k)(\mathbf{W}_{k-1} \mathbf{T}_k)^T \tag{23}$$

which yields the following iterative update equations:

$$\left.\begin{aligned} \mathbf{W}_k &= \mathbf{W}_{k-1}\mathrm{T}_k \\ \mathbf{\Omega}_k &= \tfrac{\mathbf{\Lambda}_k}{k} \end{aligned}\right\} \tag{24}$$

Equation (24) provides an iterative relation between eigen spaces at consecutive time instants. Following a similar approach as discussed in Section 2.2, the principal component values of the time series at a particular time series can be extracted as below:

$$\psi_i(k) = (W_i^T(k))(\mathbf{X}_{k_D}) \tag{25}$$

The recursively updated trajectory matrix is reconstructed by utilizing the first two signal PCs of all the D input channels as shown below:

$$\mathbf{R}_i(k) = \frac{\left\{\sum_{j=1}^{D}\sum_{i=1}^{2} W_i^j(k) \times \psi_i^j(k)\right\}}{D} \tag{26}$$

The composite signal value at k^{th} instant of time is obtained as explained in equation (12). This is subsequently utilized for TVAR modeling to track damage sensitive features in real time.

5 Proposed RSSA based framework

The overall methodology followed in the paper entails a fine blend of separate modules that detect two key ingredients: *temporal* and *spatial* damage detection, simultaneously, in a single framework. The first module deals with the temporal damage detection, where the raw acceleration data is processed by the RSSA algorithm as the data streams in real time. This accounts for an online global damage detection framework as the data is not gathered in batches to form a baseline. TVAR modeling is carried out on the updated first principal component, yielding TVAR coefficients at each instant of time. As previously explained, these TVAR coefficients are tracked online for any major and minor changes. Damage sensitive feature such as recursive ERD is utilized to further validate the instant of damage, obtained from the AR coefficients. Once the damage instant is detected, the spatial damage detection module further resolves the location of damage.

The basic steps of the algorithm are enumerated as follows:

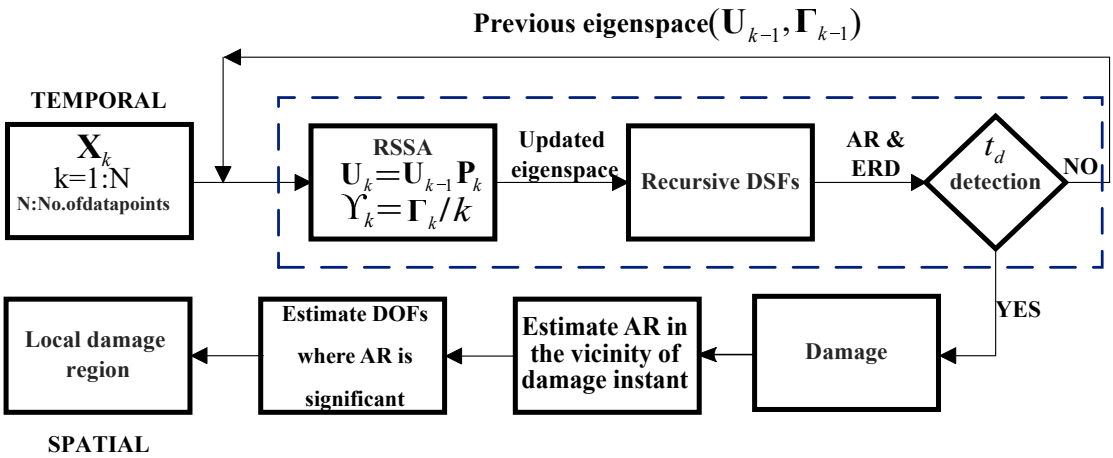

Figure 1. Basic framework of the proposed algorithm

1. First, traditional SSA is employed on some initial data points (around 100 in number) in order to estimate the initial eigen vector and eigen value matrices. The number of data points chosen here is arbitrary and considered only to stabilize the algorithm for subsequent real time damage detection.

2. The RSSA algorithm then operates online on the real time input of the streaming data. This generates a Hankel matrix out of the set of physical responses.

3. Using the recursive gain depth parameter, the covariance estimate of the Hankel matrix at the present time instant is derived using the covariance estimate at preceding time instant. From the recursive updates, the eigen vector and eigen value matrices are updated using FOP approach and the transformed responses (principal components) are obtained using the RSSA algorithm.

4. During the reconstruction phase, an approximate time series is obtained according to the relative order of significance as given by the decreasing order of the corresponding eigen values.

5. The proposed time series models are generated based on the approximated time series and a TVAR model is fit. The DSFs are tracked real time in order to extract the changes in the model coefficients, thereby revealing the faults in the system.

6. Once the instant of damage is determined, the algorithm shifts on to the next module where the spatial detection of damage takes place. DSFs are tracked online, recursively, to capture the spatial

effect of the damage. To further validate the instant of damage obtain from the AR plots, recursive ERD is utilized to show changes in the mean level at the instant of damage.

The flowchart shown in Figure 1 outlines the proposed damage detection scheme. Vibration responses are processed by the RSSA algorithm to obtain the transformed responses and TVAR modeling is utilized to extract time-varying coefficients through which damage instant is detected. It should be noted that the aforementioned proposed algorithm has the following characteristics: (**i**) the data is processed at each time instant, as and when it becomes available, i.e the algorithm works online. (**ii**) to locate the instant of damage a reference value (baseline) is not required, i.e. it is baseline free. (**iii**) there are no parameters controlling the working of the algorithm, hence its parameter free. These characteristics make it an appropriate choice for a real time damage detection framework.

6 Numerical Example

The applicability of the proposed method towards simulated models clearly exhibit the potential of the algorithm towards real time damage detection. Numerical simulations are carried out on a 4-storey structure modeled with a B-W oscillator at its base and a single-storey model with a Duffing oscillator. The global damage in the models is introduced through a change in the nonlinear force term governing the equation of motion. This is verified in the study through the use of a damage index (DI) developed by Carrillo (Carrillo 2015) and validated through hysteresis plots, described in the following sections. The variations in the hysteresis plots closely resemble to the real life occurrence of earthquakes, where the force-displacement graphs deviate due to the presence of damage. A stationary zero mean Gaussian white noise sampled at $50Hz$ for a duration of $50s$ is used. Towards this, the models are described in detail followed by the detailed analysis of the results.

6.1 Description of the 5 storey structure with B-W isolator at its base

The 5 storied structure is modeled with 4 floors having linear stiffness and a nonlinear B-W isolator lumped at the base. The model under study is adapted from Krishnan et al. (Krishnan et al. 2017a). A lead rubber bearing (LRB) isolator separates the base from the surrounding ground. The equation of motion for the system can be summarized as:

$$\mathbf{M}\ddot{X} + \mathbf{C}\dot{X} + \mathbf{K}X = \mathbf{\Lambda}F - \mathbf{M}\mathbf{I}\ddot{\mathbf{X}}_{\mathbf{g}} \tag{27}$$

M, **C**, and **K** are the assembled mass, damping, and stiffness matrices, respectively. A simple shear building representation is assumed to arrive at the expressions for **M**, **C**, and **K** as per (Krishnan et al. 2017a) which can be referred for detail. The state equations for this system subjected to an external

excitation vector W can be written as:

$$\begin{aligned} \dot{X} &= \mathbf{A}X + \mathbf{E}W \\ Y &= \mathbf{B}X \end{aligned} \tag{28}$$

Here, the vector X is the vector of states, defined as the smallest possible subset of system variables that can represent the entire state of the system at any given time. The vector Y represents the output vector, which is governed by the **B** matrix. The system matrix, **A**, and the excitation matrix **E** are given by

$$\begin{aligned} \mathbf{A} &= \begin{bmatrix} [\mathbf{O}]_{5\times5} & [\mathbf{I}]_{5\times5} \\ -\mathbf{M^{-1}K} & -\mathbf{M^{-1}C} \end{bmatrix} \\ \mathbf{E} &= \begin{bmatrix} 0 & 0 & 0 & 0 & 0 & -\frac{1}{m} & -\frac{1}{m} & -\frac{1}{m} & -\frac{1}{m} & -\frac{1}{m} \end{bmatrix}^T \end{aligned} \tag{29}$$

Numerical simulations are carried out on a simple 5 DOF mass, spring, and dashpot system. The mass at each of the four floor levels from the top is 7461 kg and at the base is 6800 kg. The damping coefficients for each floor level above the base is 23.71 kNs/m and 3.74 kNs/m for the base. The stiffness coefficients for each of the floors above the base is 11912kN/m and that for the base is 232 kN/m (Krishnan et al. 2017a).

In equation (27), $\mathbf{\Lambda}$ represents the location of the base at the point of application of the force due to the LRB base isolator and $\mathbf{\ddot{u}_g}$ represents the ground acceleration. The vector X represents the displacement of each floor and the base, with X_4 being the displacement of the top floor. It should be noted that the forces due to base damping and stiffness terms (k_b and c_b) have been included in the nonlinear force (F) due to the LRB base isolator, which can be expressed as:

$$F = \kappa z Q_{pb} + k_b X_b + c_b \dot{X}_b \tag{30}$$

where, $Q_{pb} = \left(1 - \frac{k_{yield}}{k_{initial}}\right) Q_y$ and k_b and c_b are the stiffness and the viscous damping respectively, in the horizontal direction. The term $k_{initial}$ is the initial shear stiffness and k_{yield} is the post yield shear stiffness of the LRB. The evolutionary variable z is used to provide the hysteretic component of the horizontal force, $Q_{hyst} = zQ_{pb}$. The variable z can be obtained by solving the following nonlinear differential equation:

$$z = -\gamma z \left|\dot{X}_b\right| \left|z^{n-1}\right| - \beta \dot{X}_b \left|z^n\right| + A\dot{X}_b \tag{31}$$

where γ, β, A and n are the shape parameters of the hysteresis loop (Carrillo 2015). For the current model, $A = \left(\frac{k_{yield}}{k_{initial}}\right)$, γ = β and n=1. The yield force Q_y is selected as 5% of the total weight of

the building which gives Q_y = 17800 kg and pre-yield to post- yield stiffness ratio $\left(\frac{k_{yield}}{k_{nitial}}\right) = \frac{1}{6}$. For

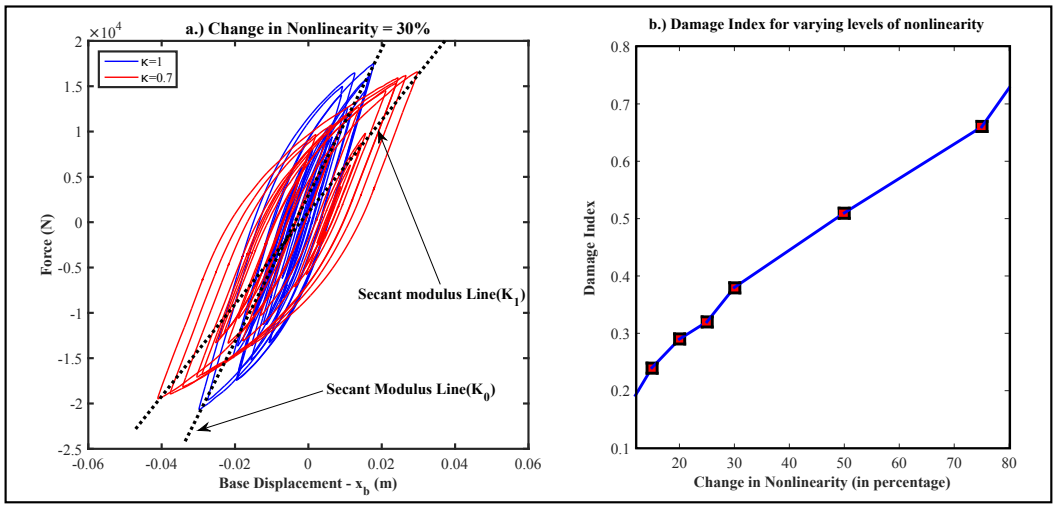

Figure 2. Force displacement variation for various levels of nonlinearity, adapted from (Krishnan et al. 2017a)

the present study of the model, γ=β=39.1. The constant κ controls the nonlinearity introduced into the equation of motion of the system (through the nonlinear force term). For instance, a change in κ from 1 to 0.4 is conveniently assumed as a 60% change in nonlinear characteristics of the system. The force induction through a change in the value of κ is considered as damage in the present context as it contributes to a change in the nonlinearity of the system. These changes to the system are permanent and do not wear over time and thus, it can be safely assumed that the damage is certainly not repaired as time progresses. The change in the nonlinear force term, κ, takes place at a particular instant of time, closely emulating a temporal damage to the system. The variations in the force-displacement characteristics replicate to instances of real life occurrence of earthquakes where the hysteresis plots deviate due to the presence of damage, thus verifying the fact that the change in the nonlinear force term induces a global damage to the structure. In order to quantitatively represent this damage, an empirical damage index (DI), developed by Carrillo (Carrillo 2015) is used in this study. The empirical DI is expressed as follows (Carrillo 2015):

$$DI = 1 - \left(\frac{K_1}{K_0}\right) \tag{32}$$

where $\left(\frac{K_1}{K_0}\right)$ is defined as the ratio between the secant modulus (K_1) associated with a changed level of nonlinearity (damaged state) to the initial secant modulus (K_0) of the pristine (undamaged) state.

The value of the index becomes zero when the ratio $\left(\frac{K_1}{K_0}\right)$ becomes unity, thereby indicating the cases of no damage to the system. The model under study has been adapted from a separate work by the authors (accepted in the Journal of Mechanical Systems and Signal Processing (Krishnan et al. 2017b)), involving the use of recursive principal component analysis (RPCA) along with TVAR in order to identify damage and its location.

6.2 Description of the single-storey modeled with Duffing oscillator

The Duffing oscillator is one of the prototype systems of nonlinear dynamics. The system has been successfully used to model a variety of physical processes such as stiffening springs, beam buckling, nonlinear electronic circuit. The source of the nonlinearity in a structural system that results in its dynamic behavior being modeled by the Duffing equation is the stiffness. In this section, a simple model involving a single storey structure with a Duffing oscillator at its base is described through the following equation of motion:

$$m\ddot{X} + c\dot{X} + k(X + \alpha X^3) = F(t) \tag{33}$$

The excitation $F(t)$ is zero-mean white noise with spectral density S_0. Solving the equation of motion numerically, the statistics of the response $X(t)$ can be obtained. The numerical values for system and excitation parameters are $k = 1$, $m = 1$, $c = 0.1$, $\alpha = 0.05$ and S_0 =1.

7 Detection results using the proposed framework

Case studies are undertaken for both global and local damage using the proposed algorithm. Temporal damage detection studies are carried out by changing the value of the nonlinear force term κ at a particular instant of time. Studies for local damage detection involve the test of detection performance for the case of MDOF system subjected to progressive decrease in floor-wise stiffness at steps of 15% for each $10s$ interval. This closely emulates the effects of a real life event (such as earthquake) over a structure where the degradation occurs through stages involving sequential reduction in storey stiffness (i.e., plastic hinge formation) that would ultimately lead to its collapse.

7.1 Temporal damage detection results

Case studies for 15% and 30% change in nonlinearity are provided in this section. As evident from literature, damages of the order of 25% have been often reported as a lower limit for vibration based damage detection (Musafere et al. 2015). However, this work successfully provides damage detection results for 15% change in nonlinearity using the real time acceleration response from a single channel as input. Since the transformed responses obtained using the RSSA algorithm are mono-component in nature, a relatively low model order (which is *2* in this paper) can be used. Although the proposed

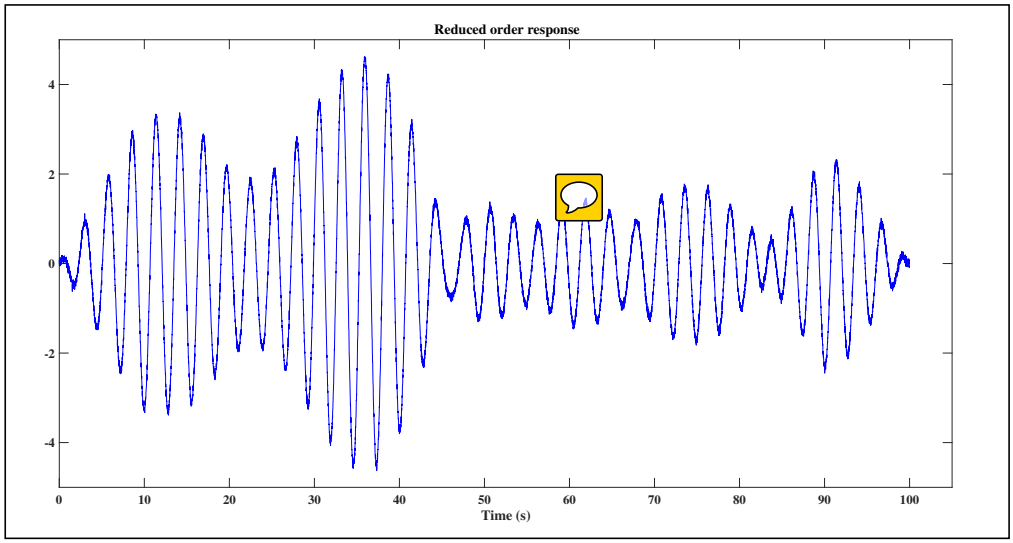

Figure 3. Plot of reduced order response

algorithm is *idealized* to provide a completely noise-free response, it could be seen from Figure 3 that the reduced order response obtained after the RSSA algorithm is not completely devoid of noise. The presence of certain noise components is evident from the distortions present in the signal. In addition, the FFT plot of the response shown in Figure 4 clearly indicates the presence of noise in the signal, thereby justifying the use of Kalman filter estimate in order to recursively update the algorithm at each time stamp. The applicability of the proposed algorithm for cases involving mean-shift over time could be well understood from the recursive mean plots of the input and output data, shown in Figure 5. It is evident from the figure that the mean of both the input and output data obtained after the RSSA module changes over time which clearly suggests that the proposed algorithm works efficiently for cases involving mean shift as well. The damage is detected using AR coefficients and ERD as DSFs shown in Figure 6 and Figure 7, respectively. From both the figures, a damage instant at $31s$ can be easily detected using AR coefficients by observing the sudden changes of the mean level of the plot. This confirms the use of TVAR modeling towards online detection of damage in a recursive framework.

To further validate the efficacy of the proposed methodology, ERD, when examined in a recursive framework, detects the instant of damage for 15% nonlinearity change at $31s$, as observed in Figure 7. While a change in the mean level of the AR plot verifies the damage instant to be at $31s$, a distinct peak

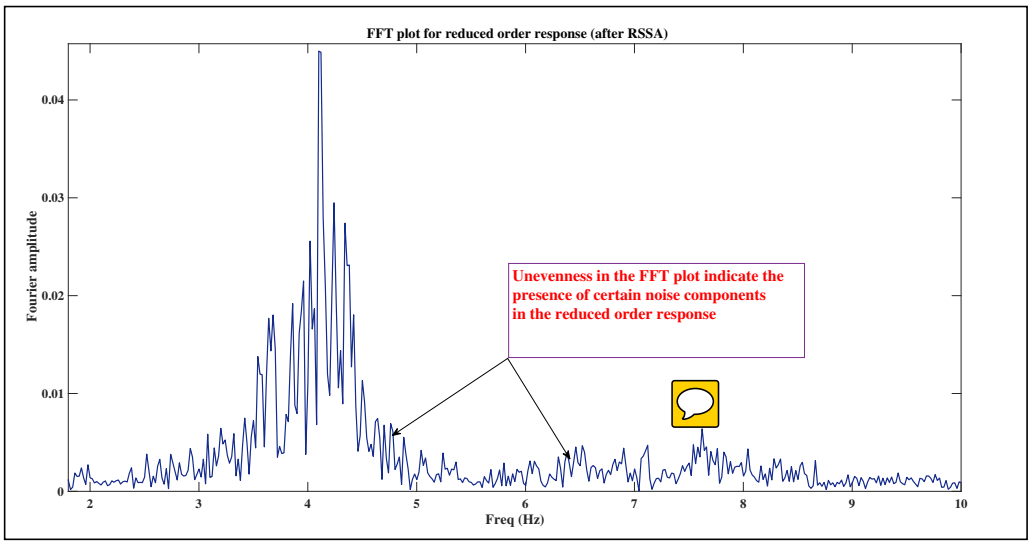

Figure 4. Noise components in the FFT of the reduced order response

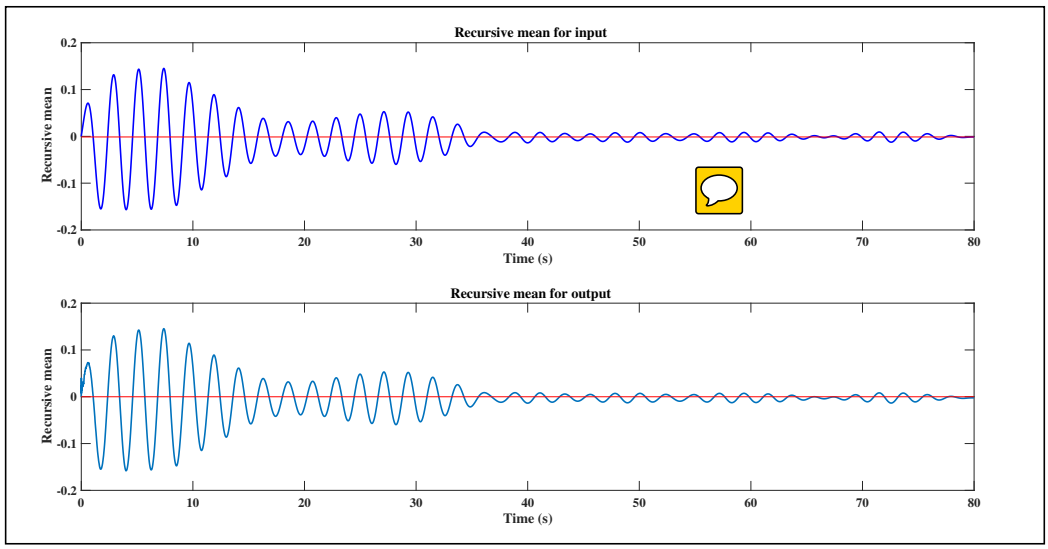

Figure 5. Mean of the input and output reduced order response

shown in the recursive ERD plots indicating the exact instant of damage further reinforces the efficacy and robustness of the algorithm.

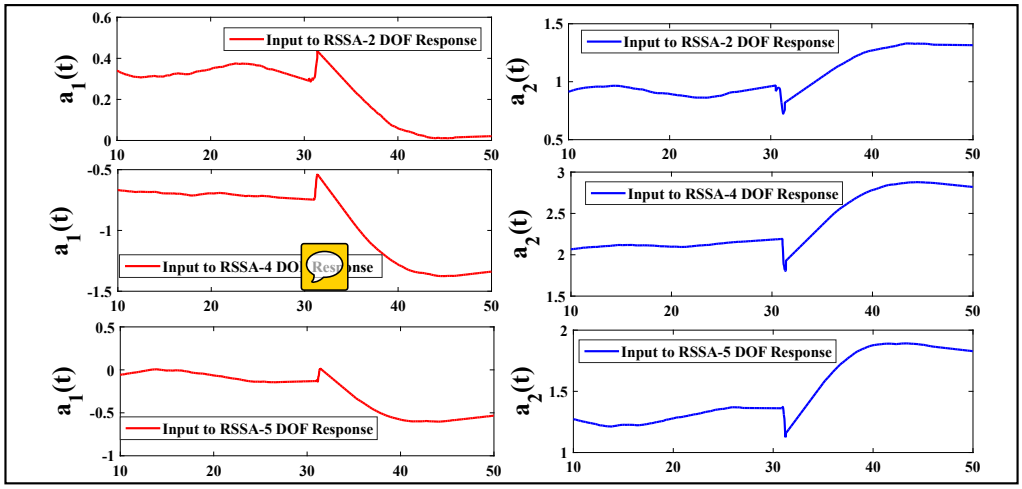

Figure 6. AR1 & AR2 plot for 30% global damage

The efficacy of the DSFs for less than 15% damage is slightly questionable which indicates that the current online framework is less reliable when the extent of damage suffered is low (i.e., less than 15%). The results are therefore, not reported here for brevity. In a separate work, the authors have recently investigated the prospects of real time damage detection using RPCA in conjunction with TVAR modeling (accepted in MSSP, (Krishnan et al. 2017b)) and have also reported global damage detection in the order of 15%. Thus, it suffices to say that both RPCA (Krishnan et al. 2017a,b) and RSSA algorithms are efficient in detecting low levels of damage in real time, but the performance of RSSA algorithm surpasses the performance of the RPCA algorithm as it takes the streaming data from a *single channel* as input, as compared to the RPCA algorithm, that requires *multi-channel* data as input. Therefore, the key novelty of the work arises due to the utilization of the streaming data available from a *single channel* that provides real time damage detection. To the best of the knowledge of the authors, this has not been reported in the literature so far.

The time taken for a single iteration of the algorithm is found to 1.18s, which closely emulates a real time process. The implementation of recursive eigenvalue decomposition consumes 10ms, which is 0.85% of the total time consumed for a complete single iteration. However, the time consumed depends upon the computational power of the system used and is more efficient for systems with superior processing power, higher gigabytes of RAM, multiple cores, etc.

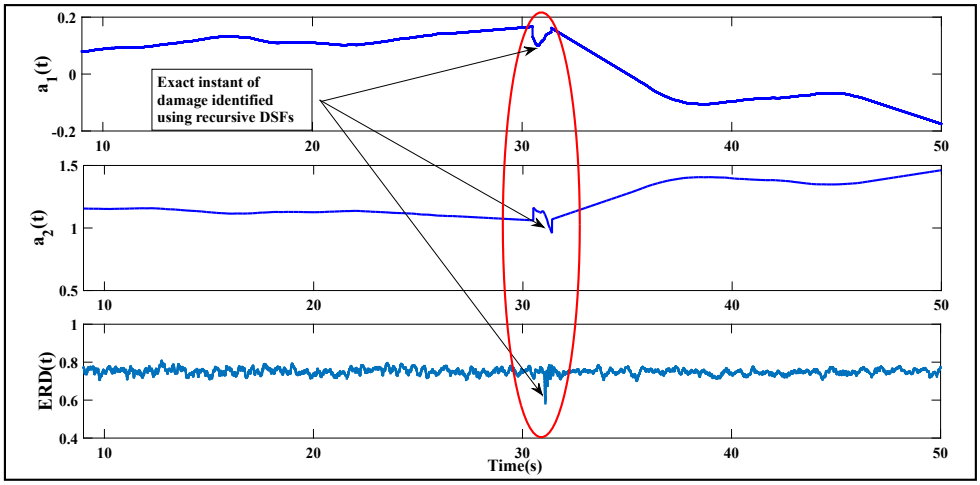

Figure 7. Recursive DSF plot for 15% global damage

7.2 Local damage detection results

In this section, the local damage detection results using the proposed algorithm is presented. The local damage is induced to the B-W model through a change in the linear storey stiffness at each floor level. The salient feature developed in the local (or spatial) damage detection scheme is consistent with events where a structure undergoes varying changes in stiffness with the progression of time, for example, during an earthquake. Case studies for successive floor-wise local damage at different instants of time are provided that are validated through the use of AR plots and ERD as recursive DSFs for real time damage detection. To this effect, the authors have carried out studies based on possible simulations closely emulating a real life event where the stiffness of each storey reduces over time.

The simulation cases considered reducing the linear stiffness of individual storey by 15% at each 10 second span. Damage was numerically induced to the fifth floor at 10 seconds from the start, to the fourth floor at 20 seconds, to the third floor at 30 seconds, to the second floor at 40 seconds and to the first floor at 50 seconds. The acceleration response from individual floor levels are provided as input to the algorithm to be processed in real time. The use of the same set of recursive DSFs for simultaneous global and local damage detection demonstrates the robustness of the proposed method. The results for local damage detection is presented next in detail.

The response from the fifth floor is provided as input to the algorithm and is processed by the recursive DSFs to indicate the local damage in the structure. From Figure 8, it can be seen that the change in the

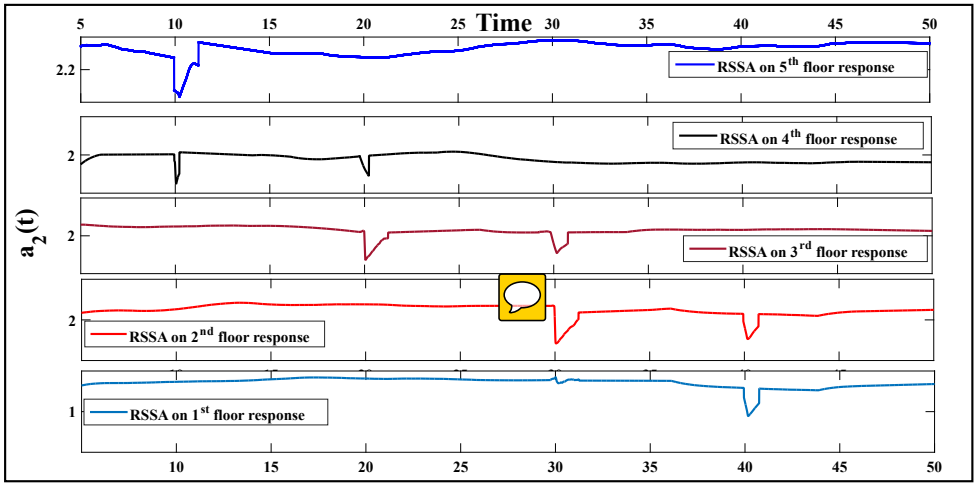

Figure 8. Local damage detection using AR coefficient - All floors

mean level of the AR plot occurs at $10s$, indicative of a linear stiffness change at that instant of time, for the fifth floor. On providing the acceleration response of the fourth floor as input for the algorithm, the sudden change in the mean level of the AR plot occurs at $20s$, that can be interpreted as a local damage. However, an additional change in the mean level could be seen at $10s$ from the start. This observation can be inferred from the fact that the fifth and the fourth floors are connected through the same column where the damage has occurred, and hence, show simultaneous peaks at both the damage instants. Similarly, the cumulative event for both the fifth and the fourth floors, clearly show that the damage has occurred to the fourth floor at $20s$ from the start of the event. Considering the response from the third floor as input for the algorithm, two peaks are observed at $20s$ and at $30s$ respectively, that indicate the progression of local damage in the structure, over time. Considering the cumulative event of the fifth, fourth and the third floor, the AR plots indicate the damage to the third floor at $30s$ through a change in the mean level of the plot.

The proposed algorithm is now applied on the response from the second storey and is processed by the set of recursive DSFs. The change in the mean level of the AR plot occurs at $40s$ from the start. As observed from the figure, the plot shows two peaks simultaneously at $30s$ and at $40s$ on considering the individual response of the second floor. However, taking into consideration the cumulative response of the fifth, fourth, third and the second floors, the local damage at the second floor can be clearly inferred from the AR plot at $40s$. The response from the first floor when provided as input to the algorithm, show change only at $40s$ from the start of the event. This result can be clearly concluded from the fact that

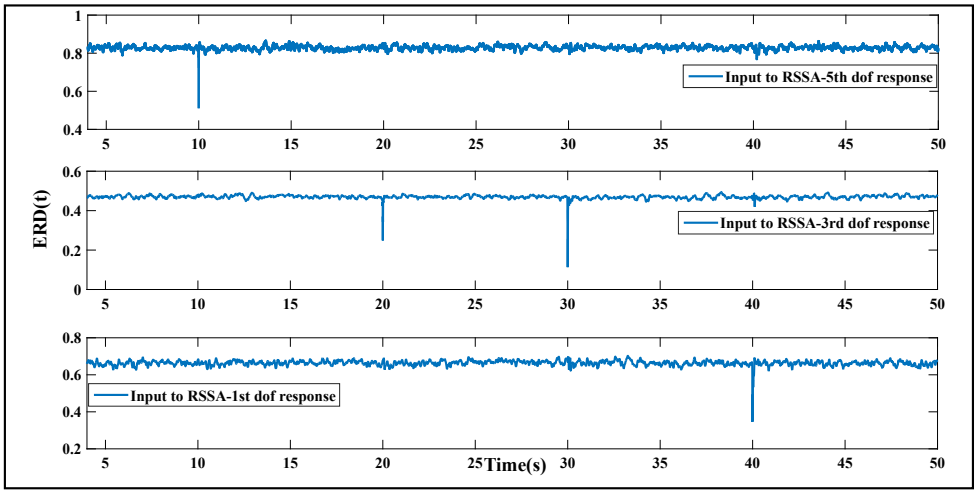

Figure 9. Local damage detection using ERD

the column connecting the second and the first floor has already suffered damage at $40s$. The cumulative event of all the floors combined indicate the damage to be at $40s$ and as the damage has stopped its progression over time, the mean level of the AR plot provide a distinctive change only at $40s$ from the start. To show the efficacy of the recursive ERD in detecting the successive floor-wise local damage, the plots of ERD for different input cases is shown in Figure 9. It can be observed from the figure that the ERD plots behave in the same manner as the AR plots for indicating the progressive damage to the structure.

7.3 Performance of the proposed algorithm against established damage detection schemes: A comparative study

In this section, the performance of the proposed method is compared with the well-established damage detection potential of the RPCA algorithm in conjunction with TVAR (Krishnan et al. (2017b)). As the proposed damage detection method is purely *online* in nature, comparison with traditional methods such as PCA, is not justified, since PCA is inherently an *offline* algorithm that requires data to be processed in batches. Windowing of the data is necessary for executing batch PCA based damage detection which prevents any possibility of online implementation of the method. A crucial point of contrast of the proposed method with the well established detection methods is the use of a *single sensor* data as input

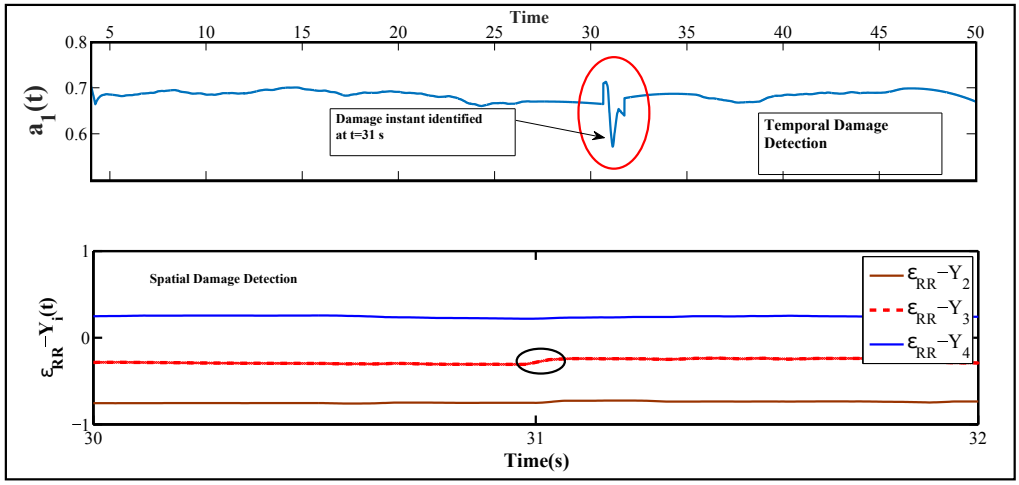

Figure 10. Comparison between spatial and temporal damage for 25% change

for damage detection process. RPCA based detection schemes use a minimum of 2 sensors as inputs for proper functioning of the algorithm. In addition, RPCA involves updating of the covariance matrix of the dataset at each time stamp, contrary to the functioning of the RSSA algorithm where the covariance update of the Hankel matrix takes place at each instant of time. In the present context, the comparative study is conducted on the B-W model described in section 6.1 under a white noise excitation of 50s duration. As evident from literature (Krishnan et al. (2017b)), the damage detection potential of the RPCA algorithm is confined to the order of 25% for spatial damage. Figure 10 clearly shows that the algorithm could effectively detect for a real-time simultaneous spatio-temporal damage of the order of 25% and that the efficacy of the RPCA algorithm for damages below 25% is slightly questionable. In this regard, the damage detection scheme proposed in this paper using the RSSA approach in conjunction with TVAR, provides better detectability of the order of 15%, as evident from section 7.2.

Thus it can be inferred from figure that the proposed algorithm based on RSSA is advantageous over RPCA based damage detection method in terms of an improved detectability of spatial damage in real time.

7.4 RMSSA results

In this section, the results showing the applicability of RMSSA towards the proposed B-W model are presented. RMSSA, an extension of the RSSA (or even the traditional SSA) approach, is effective in analyzing inputs from two or more channels from a system. The method is receptive towards temporal damage and indicates the exact instant of damage through a linear change in stiffness. At a particular instant of time, the linear stiffness of the third storey is reduced by 30%. As the third column is affected, the neighboring DOFs are expected to show distortions as discussed in section 7.2 (kindly refer Figure 8 for further details). Since the RMSSA algorithm uses multi-channel floor response as inputs at the *same time*, it cannot be used for localization of the damage that is confined only to a single storey as demonstrated in section 7.2 using multiple applications of single channel RSSA, which clearly has an advantage over the RMSSA approach for detecting local damage. Therefore, only the temporal damage detection is demonstrated in this section using RMSSA.

To this effect, response obtained from the 2^{nd} and 4^{th} floor are provided as inputs to the RMSSA algorithm. The initial signal length is selected as 6. The data processed after RMSSA is fit with TVAR models to be tracked in real time. Figure 11 provides clear detection results for a damage occurring at $31s$ through deviations in the AR plots. To further substantiate the instant of damage provided by the AR coefficients, ERD is applied over the processed data and tracked in real time, as discussed in the preceding sections. From Figure 11 (a) and (b) it can be observed that the AR plots show changes in

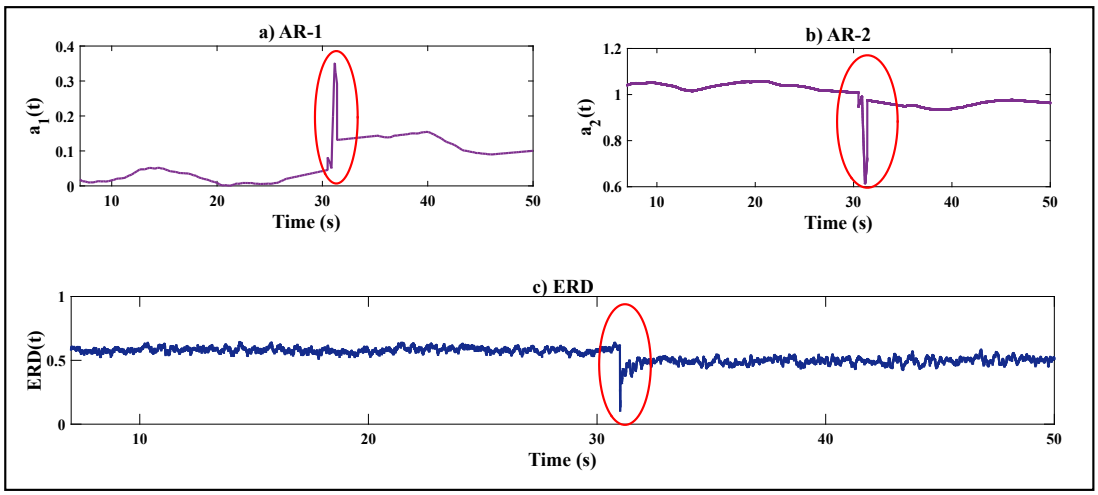

Figure 11. Detection results using RMSSA

the mean level at $31s$, precisely indicating the instant of damage. Additionally, the ERD plot (Figure 11 (c)) further validates the instant of damage to be the same as that observed from the AR plots. Thus, based on the above result, it is safe to interpret that RMSSA is consistent with RSSA towards an online implementation. The DSFs developed for the RSSA algorithm are amenable towards damage detection for RMSSA as well, showing good detection results for multi channel inputs developed towards this study.

7.5 Results for the SDOF Duffing oscillator model

The results for damage detection of the one DOF oscillator model using the proposed algorithm is presented in this section. In this approach, the acceleration response from the model is provided as input to the algorithm and is processed online to indicate damage through the DSFs. The damage is induced through a change in the α parameter shown in equation (33). The change in the parameter α is analogous to a change in the value of κ (equation (30)) that indicates an alteration in the nonlinear force term. Similar to the B-W model, the single storey modeled with the Duffing oscillator also undergoes a global damage when the force parameter controlling the effect of nonlinearity is changed at a particular instant of time. The damage is induced to the model at $26s$ from the start, through a 25% change in the nonlinear force term of equation (33).

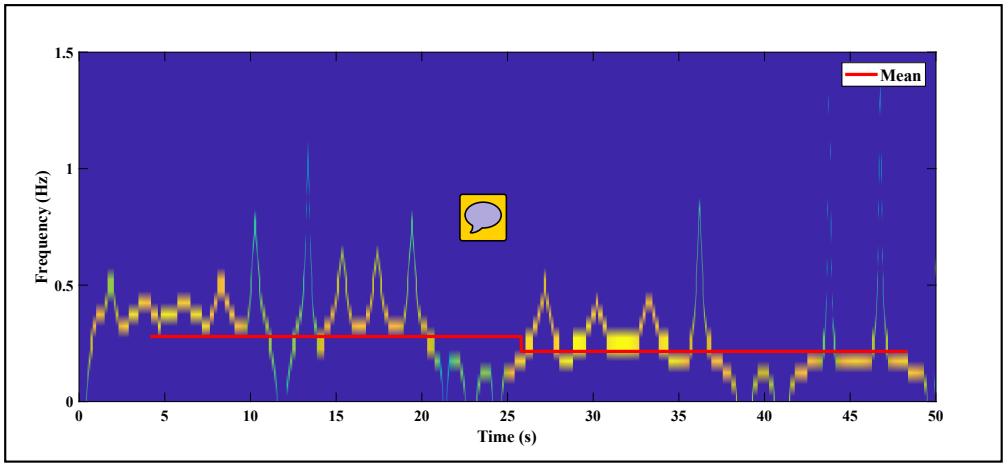

Figure 12. Hilbert Huang spectrum for SDOF Duffing oscillator

A plot of Hilbert-Huang spectrum (HHS) for the SDOF Duffing oscillator is shown in Figure 12. Empirical mode decomposition (EMD) applied to the acceleration response yields intrinsic mode functions (IMFs) (Huang et al. 1998; Yang et al. 2004; Hazra et al. 2012) for application of Hilbert spectral analysis. IMFs having significant energy content were chosen for the subsequent plotting of the HHS. The mean frequency is calculated on the basis of the average of the frequencies obtained from the instantaneous values of the Hilbert phase, considered event to event in time. Figure 12 shows the variation in the mean frequency content of the system which roughly corroborates to the changes in the system occurring due to a possible damage at a certain instant of time. A noticeable feature of the HHS is the change in the mean level of the frequency band only at $26s$, thereby, indicating the possible event at $26s$. However, it should be noted that the purpose of these plots is purely to serve as a visual aid for identifying the instant of damage and does not play any role in the real time functioning of the algorithm.

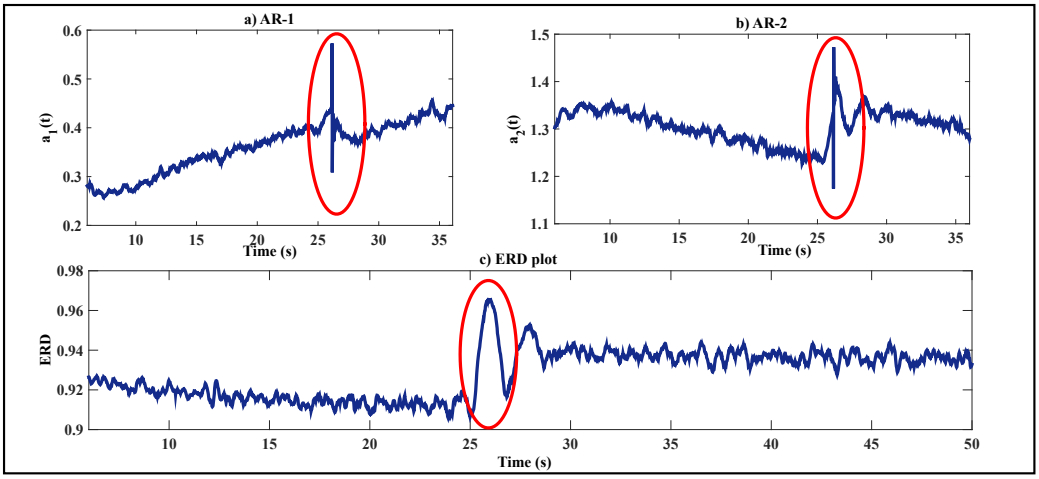

Figure 13. Damage detection for SDOF Duffing oscillator

Using the proposed algorithm, the detection results for the Duffing oscillator is shown in Figure 13. It can be observed from the figure that the plots of AR-1 and AR-2 clearly indicate an accurate damage instant at $26s$. Figure 13 (a) and (b) show a discernible change in the mean level of the AR plots at the instant of damage. A change in the mean plot verifies the efficacy of the DSF to detect damage even for a single storey structure with a nonlinear parameter associated with it. Based on these interpretations, it becomes very clear to explain the sudden change in the mean level of the ERD plot shown in Figure

13 (c). The exact instant of damage at $26s$, clearly evident from the ERD plot, further substantiates the use of the proposed methodology towards solving global damage detection problems for a category of nonlinearities that might be associated with systems.

8 Experimental verifications

Experimental studies were conducted in a laboratory environment to verify the applicability of the proposed algorithm towards solving real time damage detection problem. To substantiate the robustness of the proposed algorithm, two case studies have been presented:

1. An experimental model setup in a laboratory environment comprising of an aluminium beam excited by a ground motion, having a rubber strip attached to its free end.

2. A single degree of freedom (SDOF) system modeled as a cart attached to springs on either side of the mass experimented with a Gaussian white noise to detect damage through a change in the stiffness of the system.

8.1 Aluminium beam experiment

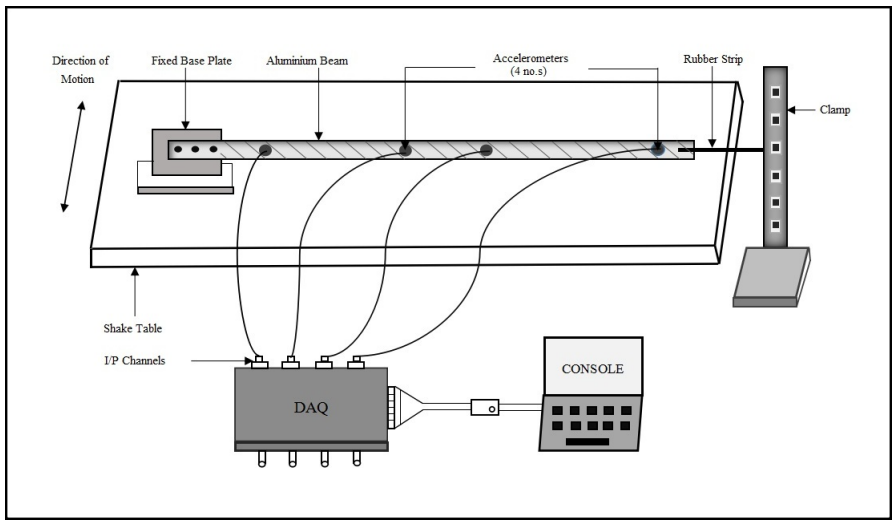

Figure 14. Details of the experimental setup (Krishnan et al. 2017a)

An experimental setup has been devised to emulate an online damage and the current algorithm has been utilized to identify the instant of damage in real time (Figure 14). The setup consists of an aluminium beam of dimension $120cm \times 3.5cm \times 0.5cm$ fixed on a base plate, drilled on top of a

shake table (model no. Bi-00-300). The base plate is a welded structure of two plates at a right-angle butt weld bearing dimensions $23cm \times 15cm \times 1cm$ each. The shake table is specified as: (i) table dimensions- $150cm \times 150cm$. (ii) payload capacity- $5tons$. (iii) peak velocity- $153cm/sec$. (iv) peak acceleration- ± 2.0 g. (v) frequency range- $0 - 20$ Hz. The model is subjected to an earthquake excitation and the acceleration data are collected using QuantumX MX410 HBM^{TM} Data Acquisition System (DAQ) at a sampling frequency of 75 Hz. The aluminium beam model is instrumented using Honeywell accelerometers $TEDS$ by HBM^{TM} at four positions. The positions of the four accelerometers from the free end are $1cm$, $30cm$, $47cm$ and $81cm$ respectively. The free end of the cantilever beam is attached with a thin rubber strip (Figure 14) which has a taut length of 70 cm and the other end of which is clamped rigidly on a heavy steel platform. This rubber strip induces a nonlinearity to the experimental setup. This model can be readily used to validate the accuracy of the proposed method as explained in the following segment.

The experiment is carried out by subjecting the aluminum beam to a scaled ground motion (1999 Chi-Chi ground motion, scaled to peak $0.3g$). In order to simulate a real time damage scenario, the rubber strip attached to the free end of the cantilever beam is snapped accurately at a fixed time instant, during the shaking motion of the beam. The measurement of the instant of the snap is done using a stop watch and the entire experiment is recorded in the form of videos to ensure accurate measurement of the instant. Although damage ideally should be an instantaneous phenomenon, the action of snapping as observed after repeated trials of experimentation takes at least *0.5* to *1*s. This small lag should be considered while calculating the damage instant. Hence, it is safe to assume that there is a possibility of a practical error of *0.5* to *1*s in recording the time of damage. Thus, the recorded time of damage should be considered as $33 \pm 1s$.

The applicability of the proposed method for cases involving mean-shifts and heteroscedastic data could be well understood from Figure 15. It is evident from the figure that the input excitation is necessarily heteroscedastic, owing to the variations at each time stamp seen from the recursive variance plot. As previously explained, the algorithm works well for cases involving mean shift as well (Refer section 7.1 for details) which is also confirmed from the plot of recursive mean that shows the evolution of the mean at each instant of time. The potential of the proposed method to detect damage for cases involving non-stationary nature of the input data could be seen from the following paragraphs that provide a detailed description of the detection results for the experimental case.

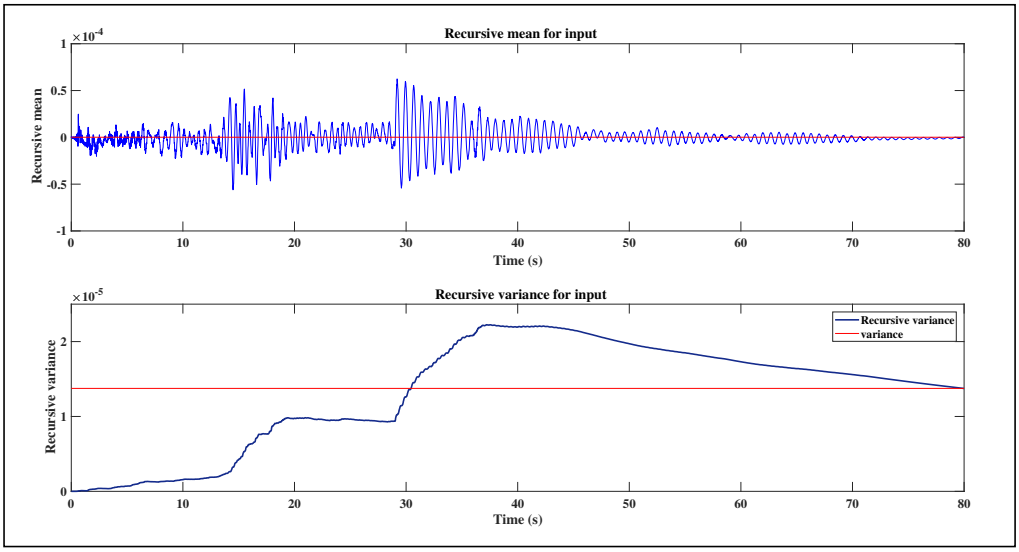

Figure 15. Recursive statistics of Chi-Chi earthquake

In order to represent the phenomena of damage for the experiment, the HHS for the present case is shown in Figure 16. As seen from the figure, a damage at $33s$ can be approximately inferred through a change in the mean level of the frequency content of the instantaneous phase. Out of the four IMFs obtained from EMD, the fourth IMF having significant energy content was used for the calculation of the HHS. As the occurrence of some background noise during the trials of the experiment is inevitable, the HHS serves as an approximate visual aid for the detection of the damage instant when supplemented with the mean frequency line. In line with most of the literature relating frequency shifts as indicators of damage (Peng et al. 2005), Figure 16 provides a reasonable first-hand representation of the damage scenario for the experimental case. As mentioned earlier, it should be noted that the implementation of these plots is purely offline in nature and are useful in providing approximate visual aids towards ascertaining damage. To further confirm the presence of damage, the data is processed through the proposed RSSA based real time damage detection algorithm which is discussed next.

The proposed algorithm is applied on the raw acceleration data streaming in real time, acquired by the QuantumX DAQ. It can be observed from Figure 17 that TVAR coefficient $a_1(t)$ shows a significant change in mean level of the plot at *33*s and persists with the same mean level till the end of the acquisition (experiment). This indicates the occurrence of damage at $33s$ which is further validated by the use of ERD

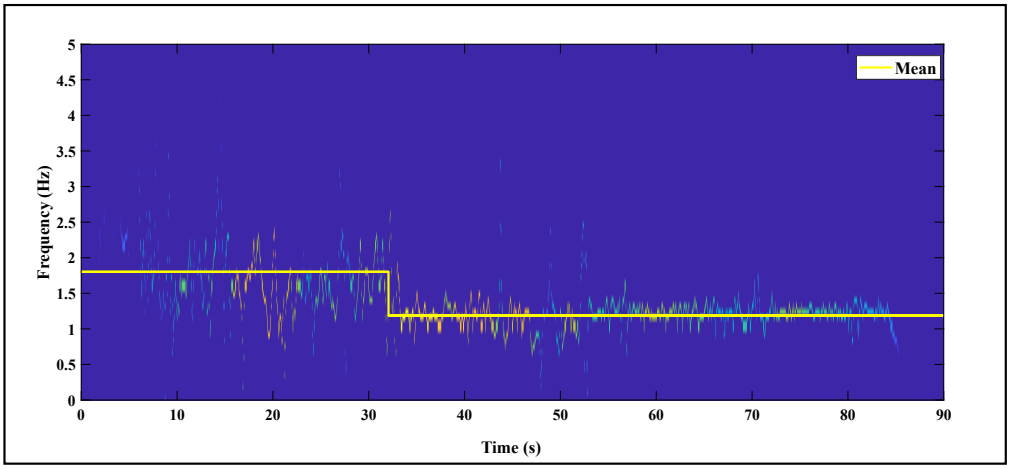

Figure 16. Hilbert Huang spectrum for the aluminium beam experiment

(Figure 17 (b)) estimated in a recursive fashion over the data set processed by the RSSA algorithm. As observed in Figure 17 (b), the peak at $33s$ clearly indicates the instant of damage. Thus, it is safe to conclude that the proposed method is effective in identifying the instant of damage in real time under experimental conditions.

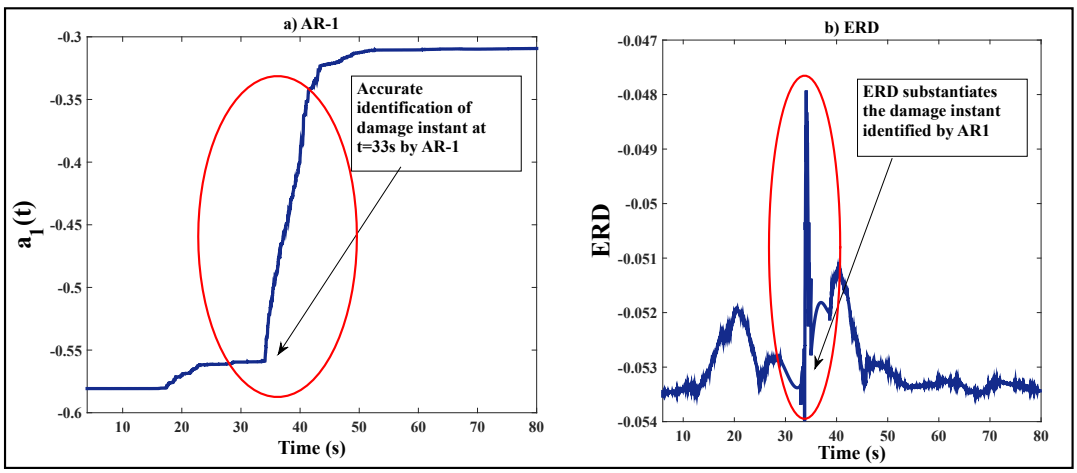

Figure 17. DSFs for the aluminium beam experiment

8.2 Toy cart experiment

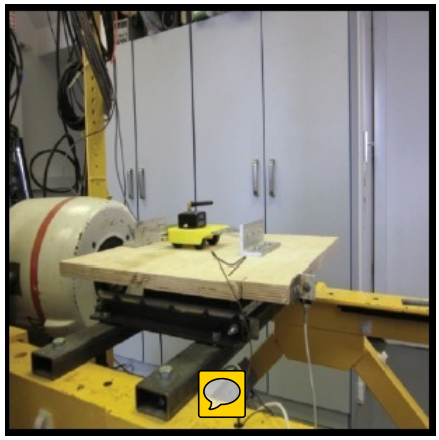

Figure 18. Setup for the toycart experiment (adapted from Pakrashi et al. (2016))

Figure 18 shows the setup consisting of an SDOF system which is physically modeled as 100g mass cart attached with three springs on either side whose other end is connected to fixed supports. The combined stiffness of the attached spring assembly is calculated as $0.379\ N/mm$. The whole setup is arranged on top of a vibration bench which is excited by an input force of suitable intensity. The structural damping is usually considerably below critical damping and the system undergoes forced vibration. While assuming the damping of the simulated model, free vibration decay of the physically built model was considered and an estimated value of 2% equivalent viscous damping ratio was used. Accelerometers placed on top of the vibration bench and the mass cart measured the input acceleration and the output response data, respectively, at a sampling rate of 830Hz. In order to ensure the accuracy of the measured data, Laser Doppler Vibrometer (LDV) attached to the cart measured the velocity of motion at a sampling rate of 128Hz, to obtain the output acceleration data through integration. Although the springs are linearly calibrated in tension under static loading and to a certain displacement, the combined system is not guaranteed to exhibit linear model behavior as obtained from linear or weakly nonlinear simulations.

The experiment is carried out by subjecting the vibration bench to a Gaussian white noise excitation and the response data sampled at a prefixed frequency. During the vibrational motion of the mass cart, the springs are carefully sheared at a particular time instant, in order to simulate a real time damage scenario (Pakrashi et al. 2016). In the present study, two damage instances are created by shearing two different springs at different time instants. The first damage instant, at $t = 13$ seconds, reduces the overall stiffness

from $0.378\ N/mm$ to $0.303\ N/mm$ (stiffness reduction of around 19%). The second break induces a stiffness alteration of around 17%, by reducing the equivalent stiffness from $0.303\ N/mm$ to $0.249\ N/mm$ at $t = 38$ seconds.

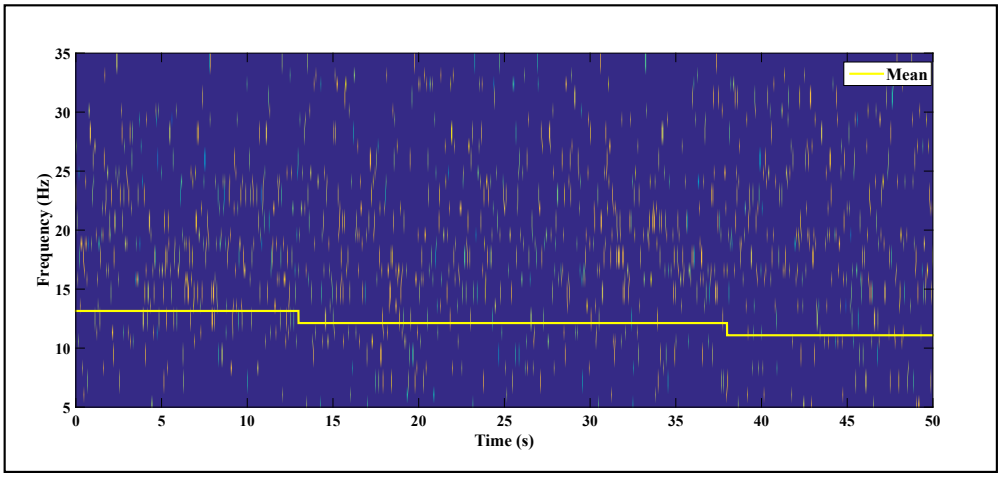

Figure 19. Hilbert Huang spectrum for the toy cart experiment

A plot of HHS showing the time varying instantaneous frequencies and the changes in the average frequency line is presented in Figure 19. The change in the average frequency is represented by the yellow line which estimates the average of the instantaneous frequencies considered event wise (i.e., from the beginning to the first shearing, first shearing to the next shearing, etc.). EMD of the acceleration responses generated IMFs, out of which the first four IMFs corresponding to the maximum energy content, were used for representing the HHS. Figure 19 shows changes in the mean level of the frequency in three stages, indicating the exact instant of shearing of the springs. Further, it can be observed from the mean frequency line that there is a change in $13s$ that continues at a steady magnitude until the point of next shearing. A change in the mean level at $38s$ approximately indicates a possible event for the experiment. However, the presence of background noise makes it difficult to discern the changes in the instantaneous frequencies themselves (without the mean frequency line), thereby rendering the visual interpretation of the HHS, difficult. To further confirm these approximate findings, detailed analysis using the proposed RSSA based framework is considered next.

The raw vibration data streaming from the accelerometer and LDV is accurately recorded at a fixed sampling rate using suitable DAQ. The proposed algorithm is applied to the acceleration data in order to identify the exact instant of damage. The damage instant is accurately identified by the DSF as observed from the Figure 20. It is clear from the figure that TVAR coefficients $a_1(t)$ and $a_2(t)$ both show changes in the mean level at the instants of damages ($13s$ and $38s$, respectively). The proposed experimental verification further validates the sensitivity of the current framework to detect structural damages as low as 17%, for a practical scenario. As clearly observed from Figure 20 (a) and (b), TVAR coefficients provide good indicators of damage for the observed damage cases. It should be noted that although the presence of noise during an experiment is inevitable, the algorithm still detects the damage instants to a fairly good level of accuracy. The successive instants of damage are efficiently captured by the recursive coefficients, indicating that the algorithm works well even for cases with multiple damage.

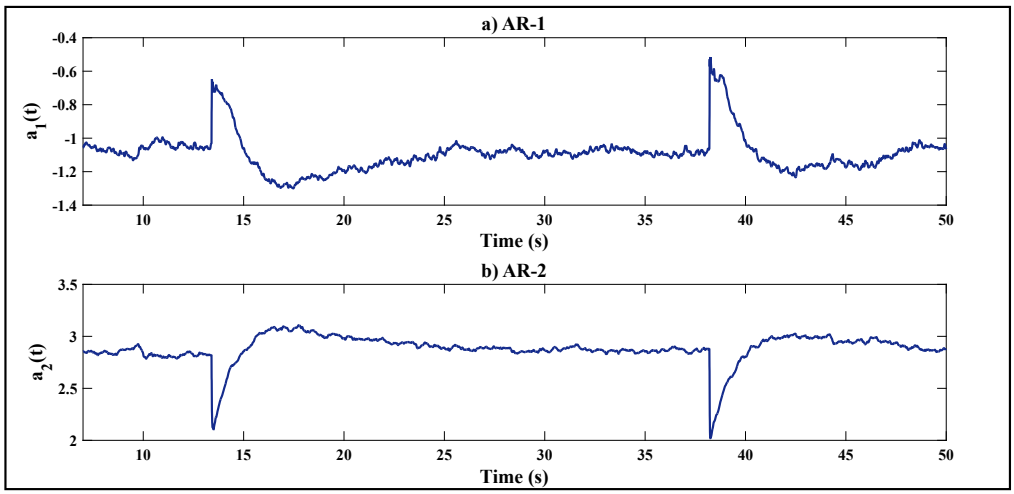

Figure 20. DSFs for the toy cart experiment

It should be noted that for slowly decaying mechanisms such as corrosion, the impact of the embedded environmental variables play a significant role in determining the accurate instant of damage, leading to an amalgamation of the original and the newer state of variables. The embedded variables need to be processed in batches using a simulated computer hard disk drive. The difficulty in measuring the real time changes in environmental and operational conditions (such as temperature, humidity, wind, etc.) arises due to cost factors, complexity in determining the optimal locations of sensors and susceptibility towards false detections of any kind. These slow varying processes hinder the applicability of the proposed

algorithm towards real time implementation and might lead to the masking of environmental variations. Thus, the proposed online algorithm might suffer from certain accuracy issues in such cases. The potential implementations of the proposed algorithm range from real time damage detection of civil structures, to data-driven mechanical and aerospace applications where the acquisition of time series data is possible. Multiple real life possibilities range from fault detection of gear boxes, detection of cracks in airplane to nonlinear damage detection in structures, instrumented with either a single sensor or even a dense array of sensors located at strategic points for health monitoring. The proposed algorithm shows effective results even for multi-channel inputs, in a recursive framework, closely emulating real life instances where the structures are subjected to low levels of damage due to external excitations.

9 Conclusions

A real time damage detection algorithm for vibrating systems based on RSSA in conjunction with TVAR model is presented. Recursive updates of the eigen subspace using rank one perturbation facilitated real time evolution of the principal components, eliciting the maximum information contained for damage detection. Subsequent modeling of principal components explaining maximum variance makes the transformed response amenable to a low order TVAR model which is a key step of the proposed framework. The use of AR coefficients as viable DSFs facilitated real time temporal damage detection for the system. The potential of ERD towards an online implementation provided substantial evidence to validate the damage instants detected through the use of AR coefficients, pitched in a recursive framework. The proposed framework provided successful detection results for damages even up to 15% for the white noise excitation and up to 17% stiffness reduction for the experimental case. RMSSA provides good detection results upto 30% linear stiffness change for a particular storey. The proposed method shows accurate damage instants through changes in the mean level of the plots for numerically simulated systems. Case studies show that the algorithm is equally capable of detecting damage online through experimental setups based on global damage schemes. The superiority of the RSSA based framework over its traditional offline version shows promising potential from a real time damage detection standpoint. The presented case studies provide evidence that the algorithm could suitably be used for real life scenarios even for single channel inputs, which is sometimes the case, considering cost and other factors. The proposed method detects damage in a recursive framework for multi channel inputs using the same set of DSFs developed for RSSA, thereby reducing computational exhaustion and extending its applicability towards a diverse range of damage detection problems. Global damage detection problems for different categories of nonlinearities associated with a system is kept as an extension of the current work to be dealt with in the future.

References

1. Znidaric A, Pakrashi V, O'Brien EJ and others (2011). *A review of road structure data in six European countries*, Journal of Urban Design and Planning, Thomas Telford Ltd. 164(4): 225–232.
2. Farrar CR and Worden K (2007) *An introduction to structural health monitoring*, Philosophical Transactions of the Royal Society of London A: Mathematical, Physical and Engineering Sciences, The Royal Society. 365(1851), 303–315.
3. Balageas D, Fritzen C-P and Güemes A (2006) *Structural health monitoring*, Wiley Online Library, vol:493.
4. Bodeux JB and Golinval JC (2001) *Application of ARMAV models to the identification and damage detection of mechanical and civil engineering structures*, Smart Materials and Structures, IOP Publishing. 10(3), 479.
5. Worden K (1997) *Structural fault detection using a novelty measure*, Journal of Sound and Vibration, Elsevier. 201(1), 85–101.
6. Balsamo L and Betti R (2015) *Data-based structural health monitoring using small training data sets*, Structural Control and Health Monitoring, Wiley Online Library. 22(10), issn = 1545-2263, 1240–1264.
7. Farrar CR and Worden K (2012) *Structural Health Monitoring: A Machine Learning Perspective*, John Wiley & Sons, Ltd. 22(10), isbn: 9781118443118.
8. Doebling SW, Farrar CR, Prime MB and others (1998) *A summary review of vibration-based damage identification methods*, Shock and vibration digest, Citeseer. 30(2), 91–105.
9. Nguyen DP, Wilson MA, Brown EN and Barbieri R (2009) *Measuring instantaneous frequency of local field potential oscillations using the Kalman smoother*, Journal of neuroscience methods, Elsevier. 184(2), 365–374
10. Yan YJ, Cheng L, Wu ZY and Yam LH (2007) *Development in vibration-based structural damage detection technique*, Mechanical Systems and Signal Processing, Elsevier. 21(5), 2198–2211.
11. Salawu OS(1997) *Detection of structural damage through changes in frequency: a review*, Engineering structures, Elsevier. 19(9), 718–723.
12. Behmanesh I and Moaveni B (2015) *Probabilistic identification of simulated damage on the Dowling Hall footbridge through Bayesian finite element model updating*, Structural Control and Health Monitoring, Wiley Online Library. 22(3), 463–483, issn: 545-2263.
13. Brownjohn J-MW, Xia P-Qi, Hao H and Xia Y (2001) *Civil structure condition assessment by FE model updating:: methodology and case studies*, Finite Elements in Analysis and Design . 37(1), 761–775, issn: 0168-874X.
14. Skolnik D, Lei Y, Yu E and Wallace, JW (2006) *Identification, model updating, and response prediction of an instrumented 15-story steel-frame building*, Earthquake Spectra. 22(3), 781–802.

15. Dackermann U, Smith WA and Randall RB (2014) *Damage identification based on response-only measurements using cepstrum analysis and artificial neural networks*, Structural Health Monitoring, Sage Publications Sage UK: London, England. 13(4), 430–444.

16. Kesavan KN and Kiremidjian AS (2012) *A wavelet-based damage diagnosis algorithm using principal component analysis*, Structural Control and Health Monitoring, Wiley Online Library. 19(8), 672–685.

17. Carden E.P and and Fanning P. (2004) *Vibration based condition monitoring: a review*, Structural health monitoring, Sage Publications. 3(4), 355–377.

18. Fan W and Qiao P. (2011) *Vibration-based damage identification methods: a review and comparative study*, Structural health monitoring, Sage Publications. 10(1), 83–111.

19. Li YY and Chen Y. (2013) *A review on recent development of vibration-based structural robust damage detection*, Structural Engineering and Mechanics, Techno-Press. 45(2), 159–168.

20. Sadhu A and Hazra B. (2013) *A novel damage detection algorithm using time-series analysis-based blind source separation*, Shock and Vibration, IOS Press. 20(3), 423–438.

21. Curadelli RO, Riera JD, Ambrosini D and Amani MG (2008) *Damage detection by means of structural damping identification*, Engineering Structures, Elsevier. 30(12), 3497–3504.

22. Pandey AK, Biswas M and Samman MM. (1991) *Damage detection from changes in curvature mode shapes*, Journal of Sound and Vibration, Elsevier. 145(2), 321 - 332. doi: http://dx.doi.org/10.1016/0022-460X(91)90595-B.

23. Yan AM, Kerschen G, De Boe P and Golinval, JC (2005) *Structural damage diagnosis under varying environmental conditionspart I: a linear analysis*, Mechanical Systems and Signal Processing, Elsevier. 19(4), 847–864.

24. Merz B, Kreibich H, Thieken A and Schmidtke R (2004) *Estimation uncertainty of direct monetary flood damage to buildings*, Natural Hazards and Earth System Science, Copernicus Publications on behalf of the European Geosciences Union. 4(1), 153–163.

25. Mottershead JE and Friswell MI (1993) *Model updating in structural dynamics: a survey*, Journal of sound and vibration, Elsevier. 167(2), 347–375.

26. Hazra B and Narasimhan S (2010) *Wavelet-based blind identification of the UCLA Factor building using ambient and earthquake responses*, Smart Materials and Structures, IOP Publishing. 19(2), 025005.

27. Hassani H (2010) *A brief introduction to singular spectrum analysis*, Optimal decisions in statistics and data analysis.

28. Golyandina N and Zhigljavsky A. (2013) *Singular Spectrum Analysis for time series*, Earthquake Engineering & Structural Dynamics, Wiley Online Library. 44(6), 831–848.

29. Elsner JB and Tsonis AA (2013) *Singular spectrum analysis: a new tool in time series analysis*, Springer Science & Business Media.

30. Misra M, Yue HH, Qin SJ and Ling C. (2002) *Multivariate process monitoring and fault diagnosis by multi-scale PCA*, Computers & Chemical Engineering, Elsevier. 26(9), 1281–1293.

31. Yu L, Zhu JH and Yu LL. (2013) *Structural damage detection in a truss bridge model using fuzzy clustering and measured FRF data reduced by principal component projection*, Advances in Structural Engineering, SAGE Publications Sage UK: London, England. 16(1), 207–217.

32. Gharibnezhad F, Mujica LE and Rodellar J. (2015) *Applying robust variant of Principal Component Analysis as a damage detector in the presence of outliers*, Mechanical Systems and Signal Processing, Elsevier. vol:50, 467–479.

33. Mirmomeni M, Lucas C, Araabi BN, Moshiri B and Bidar MR. (2013) *Recursive spectral analysis of natural time series based on eigenvector matrix perturbation for online applications*, IET signal processing, IET.

34. Golub GH and Van Loan CF. (2012) *Matrix computations*, JHU Press. vol:3.

35. Nair KK, Kiremidjian AS and Law KH. (2006) *Time series-based damage detection and localization algorithm with application to the ASCE benchmark structure*, Journal of Sound and Vibration, Elsevier. 291(1), 349–368.

36. Musafere F, Sadhu A and Liu K. (2015) *Towards damage detection using blind source separation integrated with time-varying auto-regressive modeling*, Smart Materials and Structures, IOP Publishing. 25(1), 015013.

37. Hassani H, Xu Z and Zhigljavsky A. (2013) *Singular spectrum analysis based on the perturbation theory*, Nonlinear Analysis: Real World Applications, Elsevier. 12(5), 2752–2766.

38. Liu K, Law SS, Xia Y and Zhu, XQ. (2014) *Singular spectrum analysis for enhancing the sensitivity in structural damage detection*, Journal of Sound and Vibration, Elsevier. 333(2), 392–417.

39. Chao SH and Loh CH. (2014) *Application of singular spectrum analysis to structural monitoring and damage diagnosis of bridges*, Structure and Infrastructure Engineering, Taylor & Francis. 10(6), 708–727.

40. Lakshmi K, Rao A and Gopalakrishnan N. (2016) *Application of singular spectrum analysis to structural monitoring and damage diagnosis of bridges*, Structural Control and Health Monitoring, Wiley Online Library.

41. Krishnan M, Bhowmik B, Tiwari AK and Hazra B. (2017) *Online damage detection using recursive principal component analysis and recursive condition indicators*, Smart Materials and Structures, IOP Publishing. 26(8), 085017.

42. Li W, Yue HH, Valle-Cervantes S and Qin SJ. (2000) *Recursive PCA for adaptive process monitoring*, Journal of process control, Elsevier. 10(5), 471–486.

43.Gul M and Catbas FN. (2009) *Statistical pattern recognition for Structural Health Monitoring using time series modeling: Theory and experimental verifications*, Mechanical Systems and Signal Processing, Elsevier. 23(7),

2192 - 2204.

44. Hazra B, Sadhu A and Narasimhan S. (2016) *Fault detection of gearboxes using synchro-squeezing transform*, Journal of Vibration and Control, SAGE Publications. pp:1077546315627242.

45. Carniel R, Barazza F, Tárraga M and Ortiz R. (2006) *On the singular values decoupling in the Singular Spectrum Analysis of volcanic tremor at Stromboli*, Natural Hazards and Earth System Science. 6(6), 903–909.

46. Rangelova E, Sideris MG and Kim JW. (2012) *On the capabilities of the multi-channel singular spectrum method for extracting the main periodic and non-periodic variability from weekly GRACE data*, Journal of Geodynamics, Elsevier. vol:54, 64–78.

47. Hsieh WW and Wu A. (2012) *Nonlinear multichannel singular spectrum analysis of the tropical Pacific climate variability using a neural network approach*, Journal of Geophysical Research: Oceans, Wiley Online Library. 10(7), 903–909.

48. Carrillo J. (2015) *Damage index based on stiffness degradation of low-rise RC walls*, Earthquake Engineering & Structural Dynamics, Wiley Online Library. 44(6), 831–848.

49. Pakrashi, V, Fitzgerald P, OLeary M, Jaksic V, Ryan K and Basu B. (2016) *Assessment of structural nonlinearities employing extremes of dynamic responses*, Journal of Vibration and Control, SAGE Publications Sage UK: London, England. pp:1077546316635935.

50. Groth A and Ghil M. (2015) *Monte Carlo Singular Spectrum Analysis (SSA) Revisited: Detecting Oscillator Clusters in Multivariate Datasets*, Journal of Climate. 28(19),7873–7893, doi:10.1175/JCLI-D-15-0100.1

51. Richman MB. (1986) *Rotation of principal components*, John Wiley & Sons, Ltd. 6(3), 293–335, issn: 1097-0088, doi: 10.1002/joc.3370060305

52. Venegas SA, Mysak LA and Straub DN. (1997) *Atmosphere–ocean coupled variability in the South Atlantic*, Journal of Climate. 10(11), 2904–2920.

53. Huang NE, Shen Z, Long SR, Wu MC, Shih HH, Zheng Q, Yen NC, Tung CC and Liu HH. (1998, March.) *The empirical mode decomposition and the Hilbert spectrum for nonlinear and non-stationary time series analysis*, In Proceedings of the Royal Society of London A: mathematical, physical and engineering sciences (Vol. 454, No. 1971, pp. 903-995).

54. Yang JN, Lei Y, Lin S and Huang N. (2004) *Hilbert-Huang based approach for structural damage detection*, Journal of engineering mechanics, 130(1), pp.85-95.

55. Krishnan M, Bhowmik B, Hazra B and Pakrashi V. (2017) *Real time damage detection using recursive principal components and time varying auto-regressive modeling*, Mechanical Systems and Signal Processing, Elsevier. In-press.

56. Hazra B, Sadhu A, Roffel AJ and Narasimhan S. (2012) *Hybrid Time-Frequency Blind Source Separation Towards Ambient System Identification of Structures*, Computer-Aided Civil and Infrastructure Engineering, 27(5), pp. 314–332.

57. Peng ZK, Tse PW and Chu FL. (2005) *An improved Hilbert-Huang transform and its application in vibration signal analysis*, Journal of Sound and Vibration, 286(1), pp. 187–205